Tectonophysics xxx (xxxx) xxx–xxx

Contents lists available at ScienceDirect

Tectonophysics

journal homepage: www.elsevier.com/locate/tecto

Subduction initiation in nature and models: A review

Robert J. Stern[a,*], Taras Gerya[b]

[a] Geosciences Dept., U Texas at Dallas, Richardson, TX 75080, USA
[b] Institute of Geophysics, Dept. of Earth Sciences, ETH, Sonneggstrasse 5, 8092 Zurich, Switzerland

ARTICLE INFO

Keywords:
Plate tectonics
Subduction
Lithosphere

ABSTRACT

How new subduction zones form is an emerging field of scientific research with important implications for our understanding of lithospheric strength, the driving force of plate tectonics, and Earth's tectonic history. We are making good progress towards understanding how new subduction zones form by combining field studies to identify candidates and reconstruct their timing and magmatic evolution and undertaking numerical modeling (informed by rheological constraints) to test hypotheses. Here, we review the state of the art by combining and comparing results coming from natural observations and numerical models of SI. Two modes of subduction initiation (SI) can be identified in both nature and models, spontaneous and induced. Induced SI occurs when pre-existing plate convergence causes a new subduction zone to form whereas spontaneous SI occurs without pre-existing plate motion when large lateral density contrasts occur across profound lithospheric weaknesses of various origin. We have good natural examples of 3 modes of subduction initiation, one type by induced nucleation of a subduction zone (polarity reversal) and two types of spontaneous nucleation of a subduction zone (transform collapse and plumehead margin collapse). In contrast, two proposed types of subduction initiation are not well supported by natural observations: (induced) transference and (spontaneous) passive margin collapse. Further work is therefore needed to expand on and understand the implications of these observations. Our future advancing understanding of SI will come from better geologic insights, laboratory experiments, and numerical modeling, and with improving communications between these communities.

1. Introduction

Initiation of new subduction zones through geological time is an integral part of Earth's plate tectonics regime (Bercovici, 2003; Gurnis et al., 2004; Stern, 2004; Nikolaeva et al., 2010). This key process remains enigmatic and controversial, although it is widely accepted that the negative buoyancy of sufficiently old oceanic lithosphere provides the primary driving force for subduction and plate tectonics (e.g., Vlaar and Wortel, 1976; Davies, 1999; Korenaga, 2013). It is also well understood that the bending and shear resistance of the lithosphere act against subduction initiation and in some cases may preclude development of new subduction zones (e.g., McKenzie, 1977; Nikolaeva et al., 2010, 2011). Thinking about subduction initiation (SI) has evolved gradually over the 40 years that geoscientists have been considering the problem (cf. reviews by Stern, 2004; Gurnis et al., 2004; Gerya, 2011). In recent years concepts and models of SI have evolved more rapidly as geologists, geodynamicists and experimentalists have begun working together more closely on this key problem integrating growing high-quality natural data on subduction initiation processes on the basis of more and more robust numerical geodynamical models accounting for complex properties of rocks constrained by laboratory experiments (e.g., Stern, 2004; Gurnis et al., 2004; Gerya, 2011; Hirauchi et al., 2016 and references therein). Concepts and models of subduction initiation have thus become increasingly robust and realistic in terms of the physics responsible (theory) and the resulting geochemical and rheological responses or products (evidence). This line of inquiry today is one of the most exciting fields of modern solid Earth research.

The main focus of SI-related research has evolved substantially through time. In the first fifteen years of inquiry, the focus was on compressive failure of oceanic lithosphere and was led by geodynamicists (e.g., McKenzie, 1977). Tectonic scenarios created by many geologists during this time (and continuing today) showed new subduction zones forming and disappearing willy-nilly, without attention to force balance or locations of lithospheric weaknesses. Thinking shifted in the 1990s to emphasize extensional failure of the oceanic lithosphere along transform faults and fracture zones. Key insights came from studies of oceanic forearcs and ophiolites, made possible because of technological advances in deepwater exploration and by the rise of Asian marine geosciences, especially that of Japan. Deep sea drilling at the Izu-Bonin-

* Corresponding author.
E-mail addresses: rjstern@utdallas.edu (R.J. Stern), taras.gerya@erdw.ethz.ch (T. Gerya).

https://doi.org/10.1016/j.tecto.2017.10.014
Received 7 February 2017; Received in revised form 11 October 2017; Accepted 17 October 2017

Mariana (IBM) convergent margin allowed geoscientists to study the oceanic crust of the IBM forearc. These studies increasingly pointed to seafloor spreading – strong extension – accompanying formation of the IBM subduction zone.

The recognition that extension, not compression, accompanied initiation of some intra-oceanic subduction zones was an important breakthrough, which led to clearer understanding of how these subduction zones may have started. The observed seafloor spreading on the upper plate of a nascent subduction zone suggests that the sinking lithosphere slab caused rapid trench rollback, allowing asthenosphere to flood over the sinking slab. Recognizing that some oceanic forearcs formed in this way also allowed us to better understand that certain kinds of ophiolite complexes form during SI. Further important natural evidence on the infancy of subduction and metamorphic-rheological evolution of an incipient subduction interface came from geological-petrological studies of metamorphic soles (e.g., Agard et al., 2007, 2016 and references therein). It has been demonstrated that the earliest subduction stage after SI coincides with the transient (yet systematic) transfer of material from the top of the forming slab to the upper plate, as witnessed by metamorphic soles welded beneath some ophiolites. It has been also suggested (van Hinsbergen et al. 2015) that metamorphic soles can exhume by changing mantle wedge shape during fore-arc extension caused by flattening of an anchored nascent slab advancing in the direction of the absolute plate motion. Understanding of the subduction infancy stage is thus very important since during this critical time period any newly initiated subduction zone must overcome an initial mechanical resistance and may vanish before the growing slab pull will make it self-sustaining (e.g., McKenzie, 1977; Hall et al., 2003; Dymkova and Gerya, 2013; Agard et al., 2016). In this context, empirical data on formation, exhumation and P-T-time paths of metamorphic soles marking the subduction infancy stage provide valuable constrains for testing various SI scenarios on the basis of numerical models (e.g., Duretz et al., 2016).

These robust observations and simple conclusions allowed a new generation of more realistic geodynamic models to be developed (cf. review by Gerya, 2011; Duretz et al., 2016). Such models continue to improve in the early 21st century as geologists and geodynamicists increasingly work together on developing and testing hypotheses concerning various subduction initiation scenarios for both modern and ancient conditions. However, a number of important controversies still exist in terms of the physical consistency and observational support for both “traditional” and “new” subduction initiation mechanisms (Fig. 1) proposed in the literature (e.g., reviews Stern, 2004; Gerya, 2011 and references therein). In particular, the question whether or not passive continental margins collapse remains unresolved and actively debated for both modern and early Earth conditions (e.g., McKenzie, 1977; Nikolaeva et al., 2011; Rey et al., 2014). On the other hand, recent ideas about lithospheric failure as a result of prolonged interaction with a plume head have been advanced and tested (Ueda et al., 2008; Burov and Cloetingh, 2010; Whattam and Stern, 2015; Gerya et al., 2015; Crameri and Tackley, 2016). Feasibility of further alternative SI mechanisms, such as inversion of oceanic ridges (e.g., Agard et al., 2007, 2016), has been tested numerically (Maffione et al., 2015; Duretz et al., 2016). Significant progress has also been made in terms of understanding SI from the global mantle convection prospective (e.g., Rolf and Tackley, 2011; Crameri and Tackley, 2016; Ulvrova et al., 2017).

Recent innovations made in SI research go significantly beyond the available reviews (e.g., Stern, 2004; Gurnis et al., 2004; Gerya, 2011) and require thoughtful systematization and analysis, which motivate this review. Here, we analyze how observations, concepts and models of subduction initiation mutually evolved over the 4 decades that geoscientists have been considering the problem. We first define what we mean by subduction, then review in greater detail how and why thinking about SI has evolved and finally propose possible future scientific trends and research directions.

2. Subduction and plate tectonics

Subduction initiation is a key process for plate tectonics, which is in turn the central theory of modern geophysics and geology. Among the solid bodies of the Solar System, only Earth has plate tectonics – other tectonically active silicate bodies are encased in a single rigid or internally deformable lithosphere, or “lid” (e.g., Stern et al., 2017a,b and references therein) – so special circumstances are required for plate tectonics. Plate tectonics has been formally defined as “a theory of global tectonics in which the lithosphere is divided into a mosaic of crustal plates, each of which moves on the viscous asthenosphere more or less independently to collide with, slide under, or move past adjacent plates” (Dictionary.com.). This is one of several similar definitions, all of which emphasize plate motions (kinematics) but not what powers

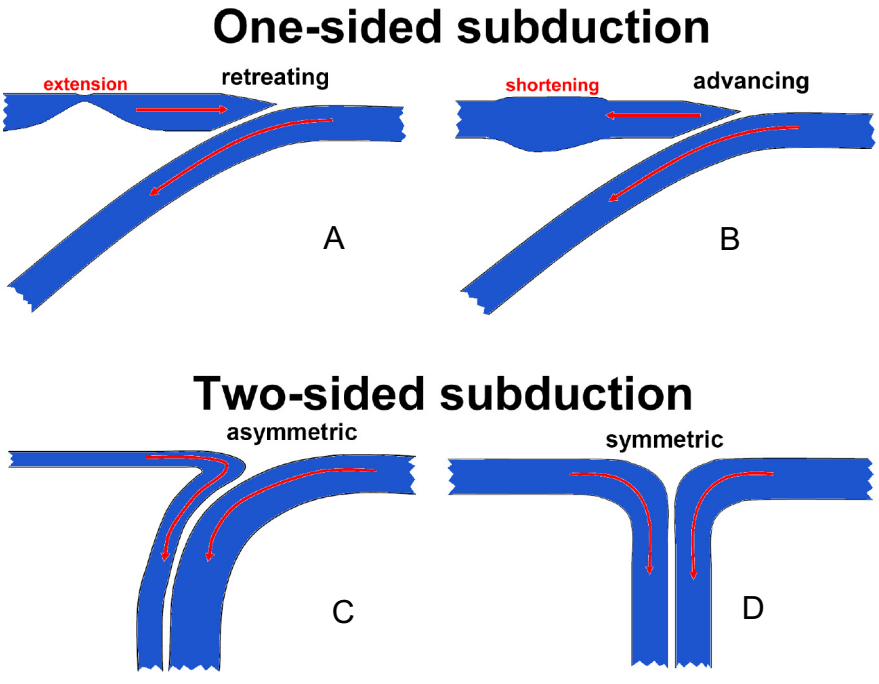

Fig. 1. Comparison of one-sided (A–B) and two-sided (C–D) subduction (Gerya et al., 2008). In case of one-sided subduction, the overriding plate does not subduct and only moves horizontally. Depending on relative plate motion, the overriding plate can be either extending (A) or shortening (B). In case of two-sided geometries, both plates subduct together. Depending on plate strength, two-sided subduction can be either symmetric (for strong plates, C) or asymmetric (for weak plates, D).

plate motions (dynamics). A theory for a phenomenon that does not also describe what causes the phenomenon is incomplete. In particular, the kinematic definition does not reveal the critical role of SI for both starting and maintaining modern-style global plate tectonics. Thus, plate tectonics needs to be redefined to include the causes of plate motion. It is widely accepted that global plate motions are mostly powered by the sinking of the negatively buoyant oceanic lithosphere in subduction zones, although a significant role of ridge push and mantle convection drag for modifying these motions has been repeatedly proposed (e.g., Becker and Faccenna, 2011; Lu et al., 2015). This breakthrough in our understanding was made by Forsythe and Uyeda (1975) and has been largely confirmed, most recently in a review by Lithgow-Bertelloni (2014). It was not always this way; in fact, plate tectonic theory was elegantly articulated by McKenzie and Parker (1967) and Le Pichon (1968) several years before the term "subduction" was introduced with its modern meaning by White et al. (1970).

In recognition of our better understanding of the process and in order to highlight the central roles of SI in modern plate tectonics theory, we start this review by updating the definition of plate tectonics to include a dynamic explanation: "A theory of global tectonics powered by subduction in which the lithosphere is divided into a mosaic of strong lithospheric plates, which move on and sink into weaker ductile asthenosphere. Three types of localized plate boundaries form the interconnected global network: new oceanic plate material is created by seafloor spreading at *mid-ocean ridges*, old oceanic lithosphere sinks at *subduction zones*, and two plates slide past each other along *transform faults*. The negative buoyancy of old dense oceanic lithosphere, which sinks in subduction zones, mostly powers plate movements." The role of the subduction process and subduction zones is thus integral in this redefinition, and a strong case could be made that "subduction tectonics" is a more accurate and thus better name for modern-style global plate tectonics. Insofar as this is true, our understanding of plate tectonics is no better than our understanding of the subduction process from its initiation to its fate.[1] It is also obvious that subduction initiation is needed to start plate tectonics at a first place.

3. Asymmetry of subduction and the strength of the lithosphere

3.1. Asymmetry of subduction

A key aspect of subduction is that it is asymmetric (one-sided subduction, Fig. 1A, B) (Gerya et al., 2008). Specifically, the subducted slab sinks, while the overriding plate moves horizontally. This contrasts with most global mantle convection models, which predict downwelling of both plates at convergent margins (two-sided subduction, Fig. 1C, D) (Tackley, 2000). Understanding how this asymmetry forms and why is it maintained is thus a key question for modern plate tectonics (Tackley, 2000; Gerya et al., 2008; Crameri et al., 2012). Gerya et al. (2008) carried out two-dimensional (2-D) numerical experiments using a mineralogical-thermomechanical visco-elasto-plastic model with free surface to understand the cause of one-sided subduction. Their numerical experiments showed that the stability, intensity, and mode of subduction depend mainly on plate strength and a zone of weak hydrated rocks above the subducted slab (Fig. 2A–C). Two-sided subduction occurs when the plates are weak (internal friction coefficient ≤ 0.1, Fig. 2A, C); in contrast, one-sided subduction – true subduction – requires strong plates (internal friction coefficient > 0.1, Fig. 2B, C) separated from the overlying mantle by a narrow weak subduction interface (Fig. 2B).

The weak interface is maintained by the release of fluids from the subducted sediments, oceanic crust, and serpentinized upper mantle as the slab sinks and is pressurized and heated. The resulting low strength of fluid-bearing subducting rocks is controlled by high (nearly lithostatic) fluid pressure, which drastically reduces the effective friction coefficient (≤ 0.05) of the solid rock matrix (e.g., Gerya et al., 2008; Dymkova and Gerya, 2013; Gerya et al., 2015; Zheng et al., 2016). The weak interplate zone localizes deformation at the interface and decouples the strong plates, facilitating asymmetric plate movement and dragging surface plates towards the subduction zone. Recently, this conclusion based on regional-scale subduction models has been extended to a planetary scale by Crameri et al. (2012), who show that a free plate surface and weak hydrated oceanic crust are essential for both creating and maintaining the subduction asymmetry and thus producing the global pattern of one-sided subduction zones on Earth (Fig. 2D). One-sided subduction can form either directly by asymmetric SI process (e.g., Gerya et al., 2008; Nikolaeva et al., 2010; Dymkova and Gerya, 2013; Gerya et al., 2015) or gradually by amplifying initial perturbations in plate bending and motion (Crameri et al., 2012). In both cases topographic loads enabled by free plate surface are crucial for both creating and maintaining the asymmetry (Crameri et al., 2012).

3.2. Strength of the lithosphere and possible origin of weak zones

It is thus clear that asymmetry of subduction geometry is intrinsically related to the dichotomy of strength and deformation distribution within the lithosphere (e.g., Gerya et al., 2008; Crameri et al., 2012): weakly-deforming plate interiors should be rheologically strong (effective friction coefficient $\gg 0.1$, strength $\gg 100$ MPa), whereas a weak localized subduction interface (effective friction coefficient ≤ 0.05, strength ≤ 10 MPa) should accommodate nearly all the deformation associated with plate convergence. Therefore, one key question is how such weak localized plate interfaces can form to enable both initiation and long-term stability of one-sided terrestrial-type subduction. Different subduction initiation models imply that the lithospheric scale weak zones should either be inherited from previous plate tectonic history (e.g., Toth and Gurnis, 1998; Doin and Henry, 2001; Hall et al., 2003; Gurnis et al., 2004; Gerya et al., 2008; Dymkova and Gerya, 2013; Maffione et al., 2015) or develop self-consistently during SI in the strong plate interior due to various rheological feedback mechanisms (e.g., Regenauer-Lieb et al., 2001; Thielmann and Kaus, 2012; Lu et al., 2015; Gerya et al., 2015).

Induced subduction initiation across a pre-existing weak zone was initially proposed by Toth and Gurnis (1998) who showed that a new subduction zone can initiate at a preexisting dipping fault zone with reasonable plate forces (on the order of 4×10^{12} N/m) if the shear strength of the inherited fault is on the order of 5 MPa or less, which is comparable to the low strength of mature subduction interfaces (e.g., Gerya et al., 2008). Such low initial strength of the fault is significantly lower than that measured for common crustal and mantle rock types. Experimental data suggest that friction coefficients of the sheet silicates that can form in the lithosphere (talc, serpentine) are significantly larger (0.1–0.60, Reinen, 2000; Reinen et al., 1994; Moore et al., 1996; Moore and Lockner, 2007) than required for induced SI (Toth and Gurnis, 1998) if no further weakening occurs. Somewhat lower effective friction coefficients (0.07–0.13) were found experimentally by Hirauchi et al. (2016) for mantle peridotites affected by hydration reactions-induced rheological weakening, which implies that such reactions should be contemporaneous with the subduction initiation process.

Further lowering of the effective friction coefficient along pre-existing hydrated faults could be related to fluids percolating through pores and fractures (e.g., Gerya et al., 2008; Dymkova and Gerya, 2013; van Dinther et al., 2013; Zheng et al., 2016). This has, in particular, been demonstrated by Dymkova and Gerya (2013) who investigated a numerical hydro-thermo-mechanical model of spontaneous intra-oceanic subduction initiation along a pre-existing hydrated transform

[1] The way that we envision that subduction zones operate can be seen in ~9 min animation "Plate Tectonic Basics 1" < https://www.youtube.com/watch?v=6wJBOk9xjto > (Stern et al. 2017a,b).

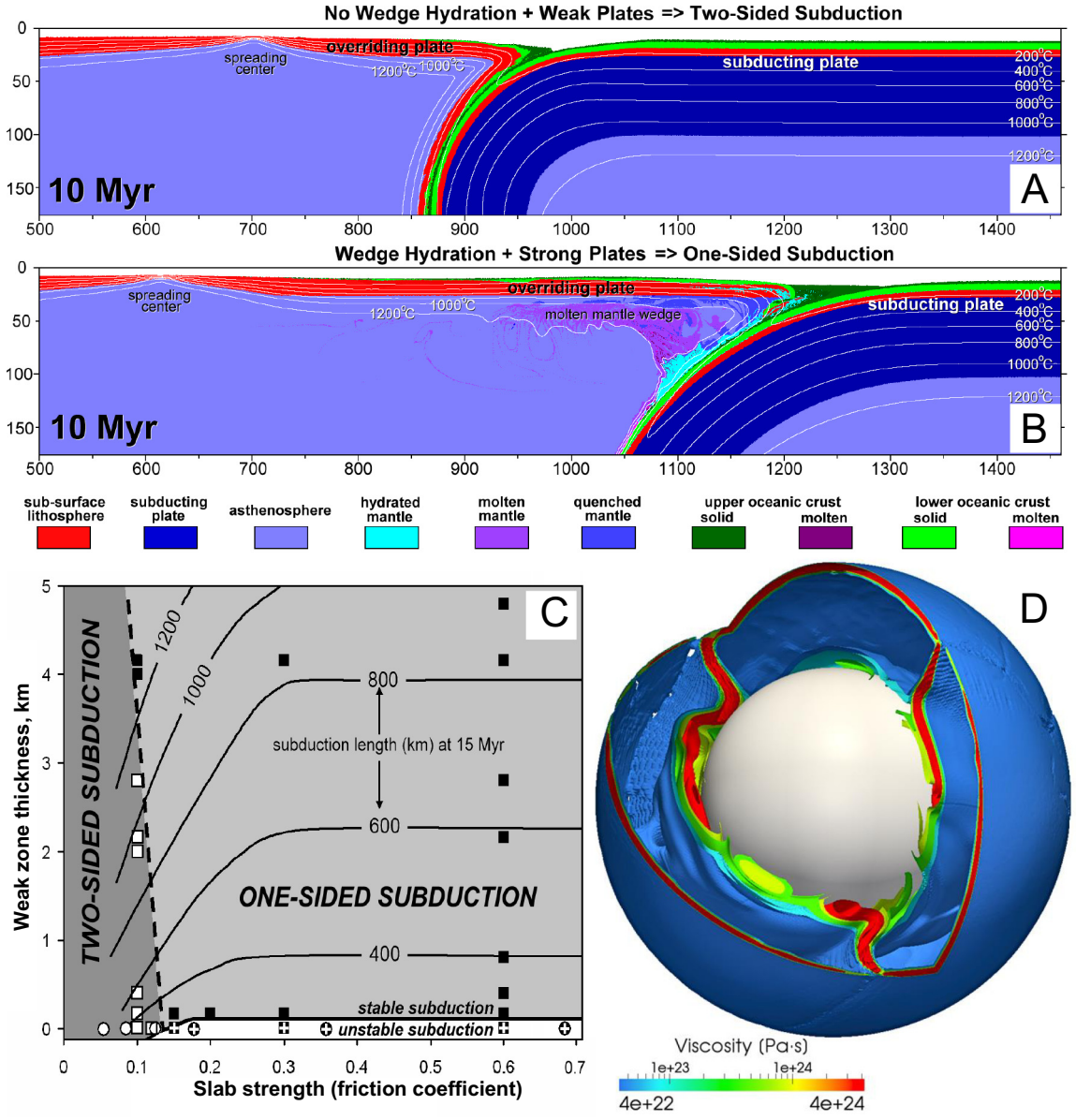

Fig. 2. Results of numerical experiments for different regimes of subduction. (A), (B) Examples of self-sustaining two-sided (A) and one-sided (B) subduction developing in regional 2D numerical experiments (Gerya et al., 2008). (C) Domain diagram showing stability, intensity, and mode of subduction as a function of slab strength and average thickness of weak hydrated rocks atop the slab (Gerya et al., 2008). Symbols correspond to conditions of numerical experiments resulting in development of one-sided (solid symbols), two-sided (open symbols) and unstable (symbols with cross) subduction regimes: squares = regional models of Gerya et al. (2008), circles = global mantle convection models of Tackley (2000). (D) Example of self-sustaining one-sided subduction developing in 3D global mantle convection model with free surface (Crameri et al., 2012).

fault. In this model with fully coupled fluid percolation and rock deformation, the experimentally measured range of friction coefficients of fault rocks (0.2–0.6) has been explored, whereas locally computed porous fluid/solid pressure ratio was used self-consistently to reduce rock strength subjected to porous fluid percolation. Dymkova and Gerya (2013) demonstrated that although subduction fails to initiate under fluid-absent conditions, it readily starts when fluid is present inside oceanic crust and along pre-existing faults. In numerical experiments, fluid percolation has been localized in the nascent forearc region along spontaneously propagating listric thrusts where high fluid pressure compensated lithostatic pressure, thus dramatically decreasing friction along the incipient subduction interface. It has been concluded (Dymkova and Gerya, 2013) that under such fluid-present conditions the lowered solid matrix permeability favors subduction initiation by maintaining high fluid pressure and thus decreasing friction along the incipient subduction interface. Dymkova and Gerya (2013) also showed that an intense overriding plate extension starts after some 10 Myr of slow subduction initiation, during which time the nascent forearc is deformed under compression whereas extension is localized within the transform fault. No spreading center forms at this slow SI stage.

Additional possible mechanisms of lowering effective strength of the incipient subduction interface include shear heating (Thielmann and Kaus, 2012; Lu et al., 2015), grainsize reduction (e.g., Bercovici, 2003; Bercovici and Ricard, 2014) and seismic weakening (e.g., van Dinther et al., 2013 and references therein). In nature, all these weakening mechanisms are likely to combine, thus leading to a composite rheological behavior of the deforming fault rocks driven by multiple feedback mechanisms. In particular, van Dinther et al. (2013) showed that seismic weakening of the subduction interface should combine with high pore fluid pressure factor (P_{fluid}/P_{solid} = 0.75–0.99) to reproduce both the long-term stability and strong seismicity of subduction zones. Recently, Bercovici and Ricard (2014) demonstrated that grain size

reduction and Zenner pinning can result in lithospheric damage, which promotes shear localization and sustaining slowly healing weak zones, thereby creating a long-lived plate mosaic in which all types of tectonic boundaries can be reused by SI.

Weakening processes are likely to be localized in both space and time but have a profound effect on the long-term behavior and effective properties of the lithosphere. Under such conditions, the effective long-term strength of the lithosphere in any given area can be defined as the average amount of mechanical work needed per unit of irreversible (i.e., non-elastic) deformation. This effective strength can be much lower than an average stress level in the lithosphere since the irreversible viscous-brittle/plastic deformation always localizes along either pre-existing or newly formed weaknesses, whereas strong blocks of the lithosphere only deform elastically (Gerya et al., 2015). One plausible example of such lithospheric weakening behavior is related to plume-induced subduction initiation (Ueda et al., 2008; Burov and Cloetingh, 2010), in which localized short-term magmatic weakening of the lithosphere along propagating dykes drastically lowers effective lithospheric strength atop the plume to 1–10 MPa (Gerya et al., 2015). This concept of the effective strength also implies that the incipient subduction interface should only weaken during brief (e.g., co-seismic) episodes of visco-brittle/plastic deformations and can stay much stronger in the long periods of quiescence associated with elastic stress buildup.

4. The ease and difficulty of making and studying new subduction zones

In the literature, there is a large spectrum of constraints and opinions concerning the ease and difficulty of making new subduction zones: predictions from simple analytical and numerical models based on experimentally defined flow laws traditionally emphasize difficulties in creating new subduction zones (e.g., McKenzie, 1977; Mueller and Phillips, 1991), whereas observations suggest frequent (yet episodic) initiation of new subduction zones in nature (Fig. 3) via a broad spectrum of SI scenarios (Fig. 4). In this respect, a key observation is that of Gurnis et al. (2004): About a third of all active subduction zones formed in the last 65 Ma, during the Cenozoic (Fig. 3). Most of these young subduction zones are of intra-oceanic origin (Dymkova and Gerya, 2013) and formed in the Western Pacific, implying that oceanic subduction initiation must be an inherent “easily and frequently” starting process of modern-style plate tectonics. This is an extremely exciting understanding, because we have a high-resolution record of plate motions during this time and so can more confidently infer the sequence of SI-related processes. This recognition leads to two additional insights: first, that SI is a relatively frequent episodic process in which the net resisting force can be overcome during the normal evolution of oceanic lithosphere; and second, that finding the geologic evidence for understanding how subduction zones formed in the Cenozoic can provide powerful insights to create realistic, quantitative and predictive global and regional SI models (e.g., Nikolaeva et al., 2011; Gerya et al., 2015; Marques et al., 2013; Crameri and Tackley, 2016; Ulvrova et al., 2017). Moreover, we have predominantly robust reconstructions of global plate motions extending back to the beginning of Cenozoic time (66 Ma) and even earlier (Müller et al., 2016), and further improving and including these would more than double the time for which examples of SI are considered. Such an extended compilation would encompass almost every convergent margin in operation today and would reward us with a greater range of examples about how new subduction zones form.

On the other hand, many difficulties exist in both recognizing and characterizing subduction initiation processes in nature. These are related to both poor data accessibility and incomplete understanding of dynamics, signatures and physical controls of SI, which can be very different from those of mature convergent margins (e.g., Hall et al., 2003; Nikolaeva et al., 2010; Marques et al., 2013; Dymkova and Gerya, 2013). Another complication is that SI happens under water, usually deep underwater, a very difficult place to study. Another source of uncertainty comes from the fact that very many (> 10) potential SI mechanisms have been proposed with only some having been systematically tested in terms of their physical consistency, controlling parameters and observable signatures (e.g., reviews by Stern, 2004; Gerya, 2011 and references therein).

5. Proposed subduction initiation mechanisms

The only classification of SI mechanisms is that of Stern (2004), who subdivided the causes of SI into *induced* (i.e., caused by ongoing plate motion, or changes in plate motion caused by changes in force balance away from the SI site) and *spontaneous* (i.e., cause by forces originating at the SI site and not elsewhere) (Fig. 4). Significant advances since then encourage the following up-to-date systematics of proposed induced and spontaneous SI mechanisms to be given.

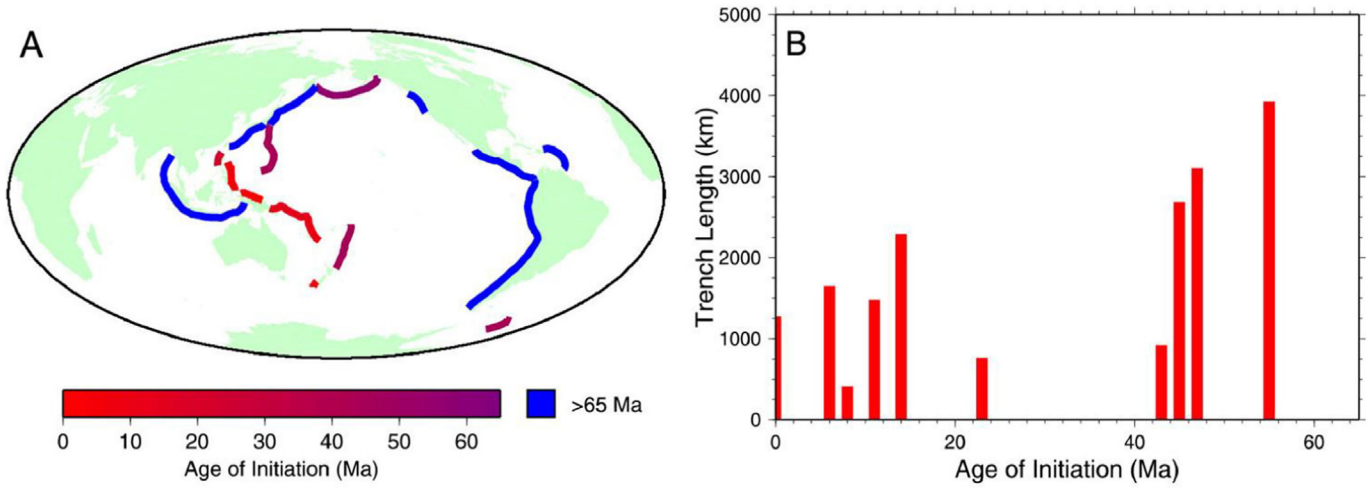

Fig. 3. Times of subduction initiation. (a) Position of present-day trenches with age of their initiation color-coded. Subduction zones that initiated before Cenozoic time are all dark purple. (b) Length of present-day trenches versus their age of initiation. Modified after Gurnis et al. (2004). (For interpretation of the references to color in this figure legend, the reader is referred to the web version of this article.)

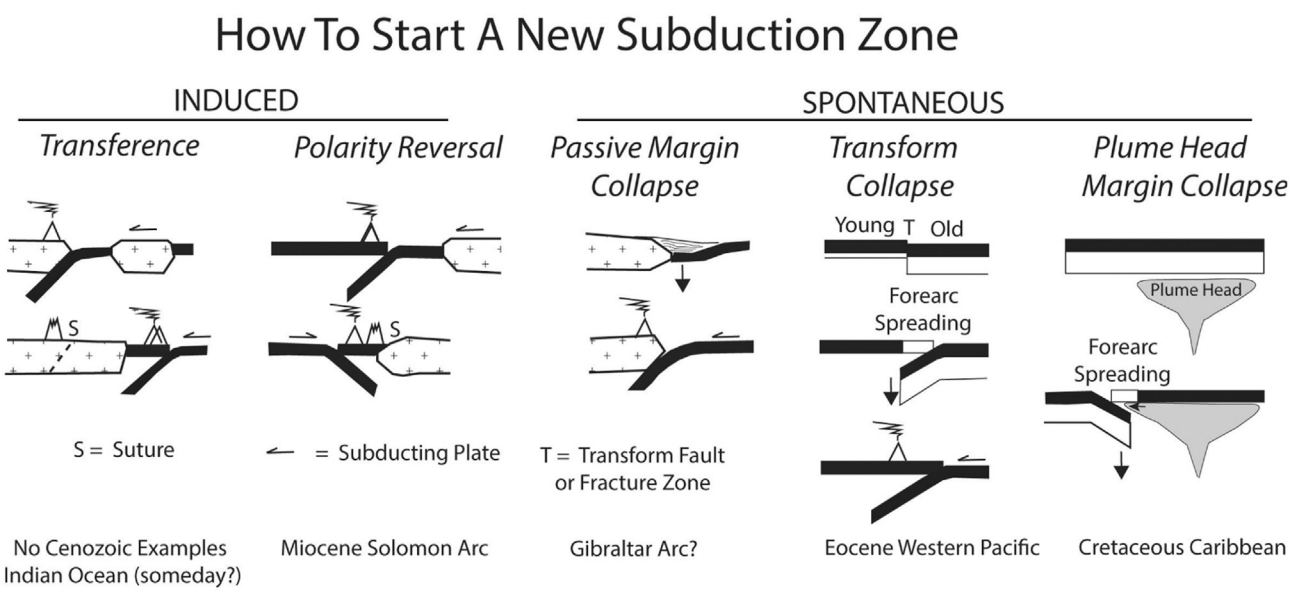

Fig. 4. General classes, subclasses and examples of how subduction zones form, modified after Stern (2004) by addition of "plume-induced subduction initiation" based on research of Whattam and Stern (2015) and Gerya et al. (2015). See Section 3 for discussion.

5.1. Mechanisms proposed for SI induced by ongoing plate motions

5.1.1. Compression-induced

- Plate rupture within an oceanic plate or at a passive margin (e.g., McKenzie, 1977; Mueller and Phillips, 1991; Shemenda, 1992), which may be caused by growth of compressional stresses associated with plate motion acceleration (Agard et al., 2007).
- Shear-heating induced localization along spontaneously forming lithospheric-scale fracture zones (Thielmann and Kaus, 2012; Lu et al., 2015).
- Subduction polarity reversal induced by attempted subduction of buoyant lithosphere (e.g., Cooper and Taylor, 1985; Pysklywek, 2001; Faccenda et al., 2008; Stern, 2004).
- Subduction zone transference (without change in the subduction direction) or "trench jump" by arc/plateau accretion (Stern, 2004; Vogt and Gerya, 2014; Tetreault and Buiter, 2012).
- Compression-induced conversion of oceanic transform faults/fracture zones/STEP (subduction-transform edge propagator) faults into trenches (e.g., Uyeda and Ben-Avraham, 1972; Casey and Dewey, 1984; Mueller and Phillips, 1991; Shemenda, 1993; Toth and Gurnis, 1998; Doin and Henry, 2001; Hall et al., 2003; Gurnis et al., 2004; Baes et al., 2011; Maffione et al., 2017).
- Inversion of spreading ridges to trenches (e.g., Agard et al., 2007; Maffione et al., 2015; van Hinsbergen et al., 2015; Duretz et al., 2016)

5.1.2. Extension-induced

- Tensile decoupling of the continental and oceanic lithosphere due to rifting (Kemp and Stevenson, 1996).

5.1.3. Mechanisms proposed for spontaneous SI

- Sedimentary or topographic loading at continental/arc margins (e.g., Dewey, 1969; Fyfe and Leonardos, 1977; Cloetingh et al., 1982; Erickson, 1993; Regenauer-Lieb et al., 2001).
- Oceanic transform faults/fracture zone collapse due to a lateral thermal buoyancy contrast between adjacent oceanic plates of contrasting ages (e.g., Karig, 1982; Matsumoto and Tomoda, 1983; Gerya et al., 2008; Nikolaeva et al., 2008; Zhu et al., 2009; Dymkova and Gerya, 2013).
- Collapse of a relic arc juxtaposed against old oceanic plate along an oceanic fracture zone (Leng and Gurnis, 2015). The collapse is driven by a combination of both thermal and compositional buoyancy contrast between the arc and the plate.
- Passive margin collapse due to a lateral thermal/compositional buoyancy contrast within the lithosphere assisted by tectonic inheritance and/or rifting and/or water- and temperature-induced weakening (Erickson and Arkani-Hamed, 1993; Kemp and Stevenson, 1996; Niu et al., 2003; Goren et al., 2008; Van der Lee et al., 2008; Nikolaeva et al., 2010, 2011; Marques et al., 2013, 2014; Rey et al., 2014).
- Small-scale convection in the sub-lithospheric mantle (Solomatov, 2004).
- Tectono-magmatic plume-lithosphere interaction (Ueda et al., 2008; Burov and Cloetingh, 2010; Whattam and Stern, 2015; Gerya et al., 2015; Crameri and Tackley, 2016).
- Large asteroid impacts (Hansen, 2009).

Due to the large variability of proposed mechanisms, an ambiguity exists about which SI concepts should be tested with observational data for each specific subduction zone and how these concepts can be tested both qualitatively and quantitatively. In order to overcome these difficulties, an iterative approach seems optimal, which incorporates observations- and concepts-inspired modeling (e.g., Regenauer-Lieb et al., 2001; Nikolaeva et al., 2010; Marques et al., 2013; Duretz et al., 2016) as well as embryonic model testing-inspired data collecting and/or (re)-analyzing (e.g., Whattam and Stern, 2015). It should also be noted that under conditions of ongoing plate motions caused by global plate tectonics some external plate forces will always be present, which may contribute to spontaneous SI scenarios (e.g., Hall et al., 2003).

Such multi-disciplinary approaches will be indeed crucial for critically analyzing various SI scenarios and identifying them in nature. For example, early thinking about forming new subduction zones by polarity reversal was supported by observations on what happened during and after Miocene collision of Ontong-Java Plateau with the Solomon Arc, which formed the New Hebrides trench and the associated N-dipping subduction zone (Cooper and Taylor, 1985). On the other hand, we have learned that there are no Cenozoic examples of subduction zone transference; in fact India has continued to collide with Asia for 50 million years rather than form a new subduction zone by

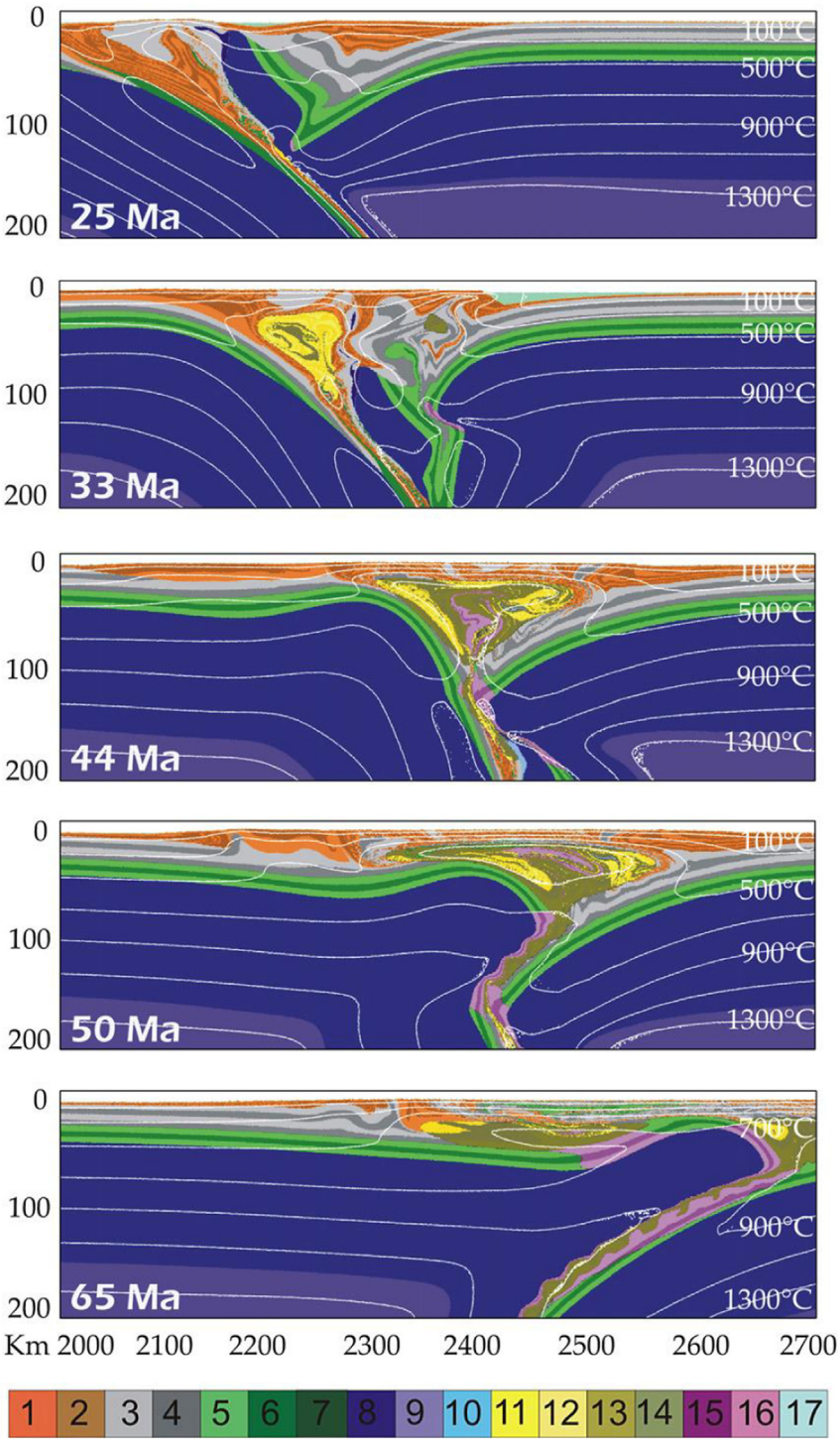

Fig. 5. Subduction polarity reversal in 2D numerical experiments for post-subduction continental collision (Faccenda et al., 2008). After the stabilization of a two-sided subduction zone, the lower slab suffers thermal weakening at the indentation zone (44 Ma). Being pushed by the imposed velocity field, the left plate starts to override the upper slab by reversing subduction polarity (50–65 Ma). The white lines are isotherms measured in °C. Color code: 1, 2 = sediments; 3, 4 = upper continental crust; 5, 6 = lower continental crust; 7 = subducted oceanic crust; 8 = lithospheric mantle; 9 = asthenospheric mantle, 10 = serpentinized/hydrated mantle; 11, 12 = partially molten sediments; 13, 14 = partially molten upper crust; 15, 16 = partially molten lower crust; 17 = seawater.

transference in the Indian Ocean. This difference between easy polarity reversal and improbable transference likely reflect the differing strengths of the lithosphere for these two different settings, but physical conditions for both transference and polarity reversals are yet to be investigated by means of systematic modeling. Some results are available for continental collision setting (e.g., Pysklywek, 2001; Faccenda et al., 2008), which suggest that subduction polarity reversal may commonly associate with building of relatively narrow symmetrical (two-sided) continental collision zones with deeply penetrating wedge-like rheologically weak lower crust decoupled from stronger subducting lithospheric mantle (Fig. 5). The results suggest that subducting mantle lithosphere is prone to detach under the collision zone, resulting in a reversal of subduction polarity; alternatively it may undergo symmetric plate consumption with gradual steepening and possible roll-over/polarity reversal (Pysklywek, 2001). Shear heating and melting of the lower crust are proposed to facilitate polarity reversal (Faccenda et al., 2008). However, applicability of these continental collision models to the arc-continent collision settings (Fig. 4) remains unexplored and requires further modeling effort.

Transference seems to be especially difficult to reproduce. Recently explored arc/plateau/terrane-continent collision models (e.g., Tetreault and Buiter, 2012; Vogt and Gerya, 2014) did not produce true transference but instead showed continued subduction of the sub-arc/plateau/terrane lithospheric mantle associated with oceanward trench

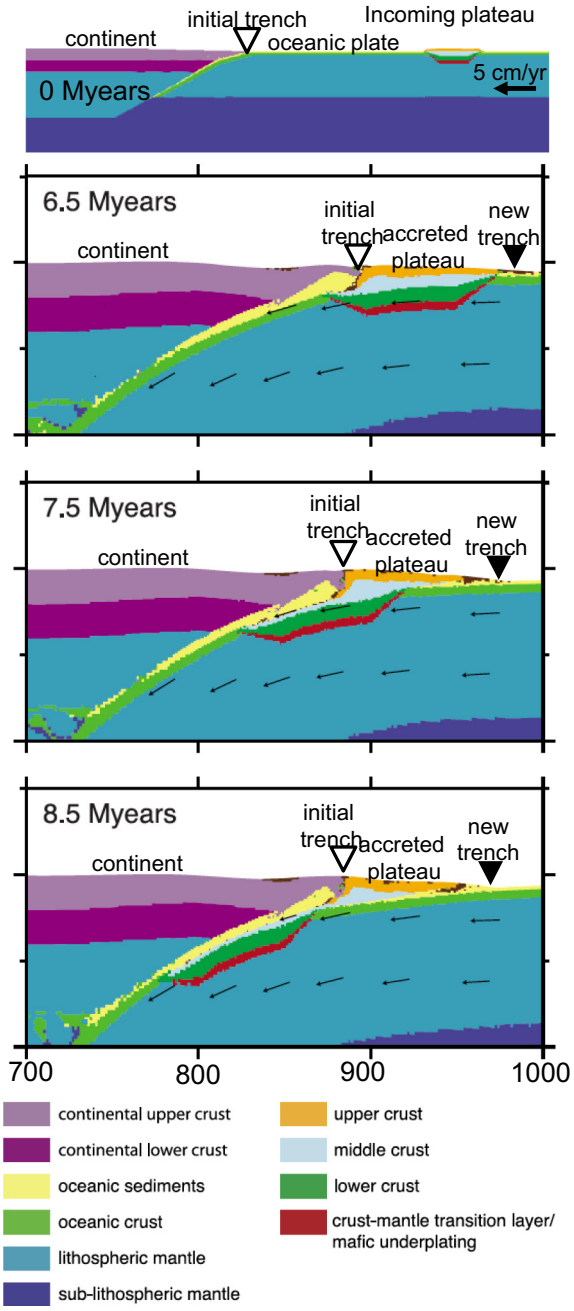

Fig. 6. Results of a numerical experiment for collision of a buoyant oceanic plateau on a subducting plate with a continent on an overriding plate (Tetreault and Buiter, 2012). At 6.5 Myr, the plateau enters the subduction zone and its middle crust becomes a region of high strain and weakens. At 7.5 Myr, the subduction channel cuts through the accreting plateau crust, and establishes itself in the middle crust. The upper crust of the plateau is sheared off into the accretionary prism area. At 8.5 Myr, the plateau crust has broken in half, with the lower crust subducting while the upper crust and parts of the middle crust remain in the accretionary prism. The new trench position is established in front of the accreted upper plateau crust. These numerical results suggest that a new subduction zone does not initiate by transference (Fig. 4) during this collision since no new lithospheric-scale fault is formed in the oceanic plate, which continues to subduct coherently.

jump and accretion of the plateau crust to the continental margin (Fig. 6). It therefore remains uncertain if true transference associated with new lithospheric-scale failure in front of accreted terrain is feasible in nature and, if so, could this be discriminated from a trench jump associated with continued subduction during arc/plateau/terrane crust accretion. It should also be mentioned that induced SI across pre-existing structures (transform faults, mid-ocean ridges, continental margins etc.) has been suggested and modeled but may be difficult to discriminate in nature from respective spontaneous SI scenarios. Accurate knowledge of topographic evolution during SI may help the discrimination: induced SI implies compression to cause failure and thus produces localized early uplift of the forearc (Hall et al., 2003), whereas spontaneous SI does not show such behavior (Dymkova and Gerya, 2013). In addition, P-T estimates for metamorphic soles (e.g., Agard et al., 2007, 2016; van Hinsbergen et al. 2015 and references therein) could be used for testing numerically (e.g., Duretz et al., 2016) the validity of spontaneous and induced SI scenarios.

6. Evolution of subduction initiation concepts and examples

One important consideration is that the subdiscipline of reconstructing subduction initiation is necessarily younger than the concept of subduction; it cannot be older than 47 years. Because this field is so young, it is not surprising that thinking about SI has not settled down yet. In spite of the youthfulness of this line of scientific inquiry, we have made a lot of progress. It is worthwhile to review how this thinking has evolved, as is done in the following paragraphs.

We can summarize how we have thought about SI according to the different distinct strands that have been advanced, each of which has dominated thinking at different times (Fig. 7). These paradigms and times begin with the Wilson cycle paradigm, which was first articulated in 1966 and continues to dominate some geoscientist's conceptions.

6.1. Early years

The first ideas of how a new subduction zone might form was implied even before the term “subduction” was adopted to explain how plate convergence was accomplished. Ideas about dipping seismic zones – what we now recognize as the signatures of subduction zones – had been evolving since the first half of the 20th century (Wadati, 1928; Gutenberg and Richter, 1938; Benioff, 1949; Coats, 1962; Isacks et al., 1968; Hamilton, 1969), but the term “subduction” was not even introduced with its modern meaning until White et al. (1970).

It took several years after articulating the modern concept of subduction to figure out how and why great slabs of oceanic lithosphere sink into the mantle, beginning at the oceanic trenches. Before this, the formation of new subduction zones was implied as part of what Burke and Dewey (1974) later called “The Wilson Cycle”. Wilson (1966) argued that Iapetus – a precursor of the Atlantic Ocean – opened in the Early Paleozoic, closed in the Late Paleozoic, then opened again in the Late Mesozoic. He envisaged nothing resembling modern conceptions of subduction zones, other than noting that “…island arcs and mountains represent places where lithosphere is being compressed, while mid-ocean ridges represent places where it is being pulled apart and where new crust is being created” (Wilson, 1966, p. 680). Wilson (1966) never thought about closing the proto-Atlantic in terms of a subduction zone, much less worried how the latter came into existence. Nevertheless, once the subduction paradigm was firmly established in the early 1970s, geoscientists began to add subduction zones into cross-section time sequences of Atlantic-type oceans opening and closing. A nebulous conception was established that new subduction zones formed inevitably at passive (rifted) continental margins during the operation of the Wilson Cycle. As we will discuss below, the formation of new subduction zones at rifted or passive continental margins is now deeply embedded in the geoscientific literature, in spite of little observational or theoretical support. Therefore, the long-standing concept of subduction initiation at passive margins requires critical thinking and quantitative testing (e.g., Nikolaeva et al., 2011; Marques et al., 2013) to avoid a risk of not being properly substantiated (cf. discussion by Dickinson, 2003 on “geomyths” — some deeply held ideas that have not been substantiated).

In the late 1970s, the geodynamic community began to attack the SI problem quantitatively. McKenzie (1977) considered the physics of the

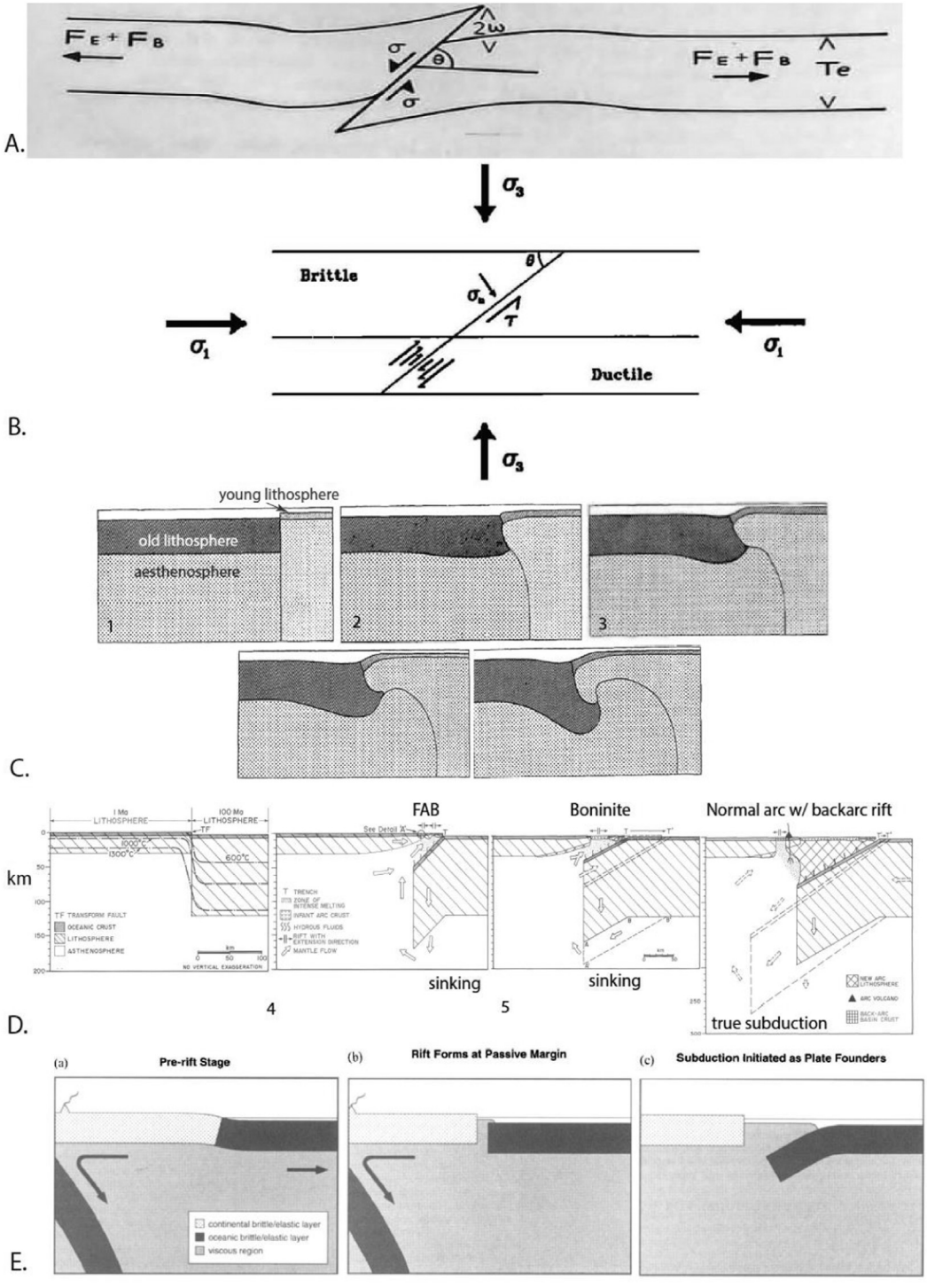

(caption on next page)

process from the point of view of a plate under compression (Fig. 7A). McKenzie (1977) estimated the minimum force required for a finite instability of the oceanic lithosphere to grow sufficiently to allow SI, concluding that this would be difficult, but not impossible. This seminal contribution strongly influenced geodynamic thinking about subduction initiation for many years (e.g., Mueller and Phillips, 1991; Toth and Gurnis, 1998; Doin and Henry, 2001; Hall et al., 2003; Gurnis et al., 2004). All but a few (e.g., Matsumoto and Tomoda, 1983; Regenauer-Lieb et al., 2001) quantitative geodynamic examinations of SI during these early investigations started with the assumption that compression was needed to rupture oceanic lithosphere to start a new subduction zone. A similar approach was followed by Mueller and Phillips (1991), who carried out a more systematic, but similar, analysis to McKenzie (1977). Their model setup is shown in fig. 7B. Mueller and Phillips (1991) assumed that pre-existing faults nearly follow Byerlee's law and have shear stresses substantially > 100 MPa. In most cases, the force necessary to overcome the strength of the lithosphere would be nearly an order of magnitude greater than likely geologic stresses. Mueller and Phillips (1991) also concluded that, under compression, subduction would be almost impossible to initiate; this conclusion remains pertinent in efforts to understand why transference and passive margin collapse do not seem to happen.

Fig. 7. Subduction initiation models, 1977–1996. A) The forces which resist SI arise through friction on the plate boundary and the need to bend both plates if subduction is to continue (McKenzie, 1977). B) Geometry of shear resistance along an incipient fault plane within normal oceanic lithosphere (Mueller and Phillips, 1991). Principal tectonic stresses are represented by σ_1 and σ_2, the resultant normal and shear stresses as resolved along the fault plane by σ_2 and τ and resultant normal and shear stresses as resolved along the fault plane indicate that relative motion is accommodated by distributed deformation. C) Results of numerical experiments on upper mantle flow at fracture zones based on density structure (Matsumoto and Tomoda, 1983). No external forces are applied, only body forces from old, dense lithosphere adjacent to young, buoyant lithosphere. 1 = model set up; 2 = situation after 12 Ma; 3 = 21 Ma, 4 = 31 Ma, 5 = 47 Ma. Notice slow deformation of the originally vertical interface. D) Spontaneous collapse along a transform fault to cause new subduction zone to form the Izu-Bonin-Mariana arc in Western Pacific (Stern and Bloomer, 1992). Section perpendicular to the transform fault/trench through the crust and upper mantle just prior to (1), and just after (2), initiation of subduction. (3) Section perpendicular to the arc showing why spreading in the forearc might cease. Original lithosphere and mantle motions are outlined in solid lines, whereas the new position and motions are outlined by dashed lines. (A) Continued subsidence of lithosphere results in fore-arc extension, with the trench moving from T to T′ as the base of the lithosphere moves from A to A′. Retreat of subsidence hinge from T to T′ involves removing asthenospheric material in trapezoid AA′BB′; further retreat involves removal of material progressively farther from the tip of the lithosphere (at B′), while progressive subsidence (from A to A′, and beyond) increasingly cuts off the route of asthenospheric transfer (shown by arrows). (4) Eventually, lithosphere begins to move with a downdip component and true subduction begins. This results in a greatly reduced rate of trench migration, which leads to a corresponding reduction in extensional stress and re-organizes flow in the mantle wedge, allowing the forearc to cool and form thick lithosphere, forcing the magmatic axis to migrate away from the trench. Extensional strain resulting from trench rollback (T′–T″) is taken up in back-arc spreading. E) Subduction initiation scenario at a passive continental margin of Kemp and Stevenson (1996). Surficial layers represent the brittle/elastic portion of the lithosphere that can support stresses on long time-scales. (a) A plate comprising continental and oceanic lithosphere with a flexed passive margin experiences basal tractions associated with subduction and sea-floor spreading. (b) Shear stresses exceed the shear strength of the margin under tension arising from the margin's slope and basal tractions. The oceanic and continental lithosphere decouple, leading to rifting. (c) A gravity current flows onto the old seafloor causing it to flex downwards and founder.

Alternative ideas for SI began to be explored by geodynamicists in the early 1980s. A particularly seminal contribution was made by Matsumoto and Tomoda (1983), who for the first time explored spontaneous subduction initiation by lithospheric flow across fracture zones offsetting old and young oceanic lithosphere (Fig. 7C). They noted that the difference in adjacent lithospheres would result in several 10s of km offset at the lithosphere-asthenosphere boundary, concluding that this would cause significant lateral forces at the boundary, which would flow and perhaps evolve into a subduction zone. They only considered differences in density between the two lithospheres (older lithosphere being significantly thicker than young lithosphere, along with density and viscosity differences between lithosphere (3.3 g/cm^3, 10^{22}–10^{23} Pa/s) and asthenosphere (3.2 g/cm^3, 10^{19}–10^{21} Pa/s). The numerical solution was based on stream function formulation combined with marker in cell approach — an advanced numerical geodynamic modeling technology, which was in many senses ahead of its time. In particular, these early models used free upper surface implementation based on “sticky water” approach, which became widespread two decades later (e.g., Gerya and Yuen, 2003; Gerya et al., 2008; Schmeling et al., 2008; Crameri et al., 2012; Crameri and Tackley, 2016).

6.2. Izu-Bonin-Mariana scientific drilling

A key conceptual breakthrough in understanding SI came as an unexpected result of scientific drilling in the Izu-Bonin-Mariana intra-oceanic convergent margin south of Japan by the Deep Sea Drilling Project (DSDP) and Ocean Drilling Project (ODP). Prior to DSDP Leg 60 drilling, it was thought that forearc crust was trapped when a new subduction zone formed (Dickinson and Sealey, 1979). Leg 60 results disproved this hypothesis, as summarized by Hussong et al. (1982, p. 9): “The principal petrologic conclusions we derive from all these sites are that igneous basement in the fore-arc trench region is primarily arc-related, extends to very nearly the trench-slope break, and probably crops out in the upper trench wall.” Natland and Tarney (1982, p. 877) elaborated: “The earliest Eocene arc was built up dominantly of arc tholeiite and boninitic lavas, with lesser calc-alkalic lavas, based on the results of Leg 60 drilling at Sites 458 and 459 in the forearc region; Leg 59, Site 448, on the Palau-Kyushu Ridge; and exposures on the islands of Palau, Guam, and Saipan. Near Sites 458 and 459, the forearc crust is thin, formed entirely under water, and includes no known component of [normal] ocean crust. Nevertheless it has many of the features of an ophiolite, produced *in situ* by earliest arc volcanism.” Natland and Tarney (1982, p. 895) went on to “… propose that Mariana fore-arc region is an *in situ* ophiolite succession with appropriately thin crust, a reasonably typical velocity structure …, and the necessary upper pillowed extrusive sequence overlying appropriate plutonic rocks. It was produced during the early stages of arc volcanism and is not a fragment of [trapped] ocean crust” (brackets are ours).

Boninites were a big part of the exciting story that came out of DSDP Leg 60. A few years earlier, Dietrich et al. (1978) reported the composition of igneous rocks dredged from the Mariana Trench during a 1976 cruise of the Dmitry Mendeleev and noted the presence of boninites, a volcanic rock type that had first been described from the Bonin (Ogasawara) Islands to the north. Boninites are an unusual volcanic rock that is rich in both MgO and SiO_2, essentially an ultramafic andesite. The unusual composition of boninites formed by partial melting of depleted mantle harzburgite that was metasomatized by fluid-mobile elements (e.g., Rb, Ba, K). Boninites are found almost exclusively in the fore-arcs of intra-oceanic arc and in ophiolite complexes thought to represent former fore-arc settings (although some boninites form in unusually depleted backarc basins, e.g. Resing et al., 2011). As the petrological community became increasingly interested in boninites through the 1980s, it became clear that an unusual tectonic setting was responsible for their formation, and that this setting could be spatially and temporarily linked to the formation of a new subduction zone.

Understanding where and how boninites formed also is key to understanding the tectonic significance of what Pearce et al. (1984) called “supra-subduction zone (SSZ) ophiolites”. Pearce et al. (1984) noted that SSZ ophiolites differ from ‘MORB’ ophiolites – those formed at a mid-ocean ridge – not only in the chemical composition of their volcanic sections but also in the more depleted nature of their mantle sequences. Pearce et al. (1984) noted that most of the best-preserved ophiolite complexes are SSZ-type and interpreted these to have formed during the initial stages in the evolution of a new subduction zone.

Ocean Drilling Project Leg 125 in the Izu forearc in 1988 provided further important insights. Site 786B was especially useful, as it was the first deep penetration of the Eocene basement of the Izu-Bonin outer-arc high, recovering 650 m of boninite flows and hyaloclastite, andesite-dacite flows, breccias, sills, and dikes (Fryer and Pearce, 1992). This drillsite showed that boninite was a common component of the Eocene IBM forearc and thus a key part of the IBM SI story.

Stern and Bloomer (1992) reconciled the petrologic evidence of strong extension that had been amassed in the previous 15 years for the earliest stages in the evolution of the IBM convergent margin by proposing a model whereby the IBM forearc formed by seafloor spreading above a sinking Pacific plate. The IBM trench formed above a great transform/fracture zone (Fig. 7D first panel) separating old, thick, dense Pacific lithosphere from young, thin, buoyant lithosphere around the Central Philippine Basin spreading ridge. This fault served as a long lithospheric weakness that allowed the two plates to move independently. At some critical point in space and time, Pacific lithosphere sank enough to allow asthenosphere to flow over it (Fig. 7D, 2nd panel). Decompression melting accompanied asthenospheric upwelling, much like that beneath mid-ocean ridges. This produced MORB-like tholeiites, what Reagan et al. (2010) call fore-arc basalts (FAB), which

show very little evidence of fluids derived from the top of the sinking lithosphere. The old lithosphere continues to sink and asthenosphere continues to flow over it, leading to further decompression melting (Fig. 7D, 3rd panel). After some time, fluids from the sinking lithosphere are able to rise through the overlying hot mantle and reach the zone of melt generation, causing already depleted mantle to melt further and imparting a strong signature of fluid-mobile trace elements to the magmas; some of these are boninites, although boninites do not always accompany SI magmatism. At some point as the old slab sinks, it starts to move down-dip, not just vertically (Fig. 7D, 4th panel). This peculiar slab dynamic during (presumably spontaneous) SI needs further detailed investigation and modeling, along the lines carried out by Zhou et al. (2016), but there could be several contributory causes, including: 1) growing length and thus overall negative buoyancy of subducted slab augmented by basalt ≥ eclogite phase transition, which increase slab pull and favor more downdip motion; 2) as the slab sinks beneath the top of the asthenosphere, it encounters increasingly viscous mantle, which may resist slab vertical motions, favoring downdip sinking instead; and 3) as slab vertical sinking progresses, it is increasingly difficult for underlying asthenosphere to move around the sinking and steepening slab, easier if the slab sinks edgewise.

Subsequent studies have built on this model, adding details, uncertainties, and complications. The recognition of Reagan et al. (2010) that early IBM SI magmas are tholeiitic FAB and later ones are boninitic was an important refinement, which was further strengthened by successfully coupled geodynamic and petrogenetic modeling (Leng et al., 2012). Further insight was provided from the recognition of two types of peridotites in the IBM forearc, as indicated by two types of dunite: (1) those with high-Cr# (Cr / (Cr + Al)) > 0.8) spinels and (2) those with medium- Cr# (0.4–0.6) spinels, both associated with harzburgite. These two groups of spinel compositions are interpreted as melt channels for two distinct melts: a boninitic melt in equilibrium with high-Cr# spinel dunite and a mid-oceanic ridge basalt (MORB)-like melt in equilibrium with medium-Cr# spinel dunite. Morishita et al. (2011) concluded that the wide range of variation in spinel Cr#s in IBM forearc dunites probably reflects changing melt compositions from MORB-like to boninitic due to increased slab-derived hydrous fluids and/or melts during the course of subduction initiation.

Another important point is that SI by transform collapse is a 4-D process (Fig. 8) and the simple cross-sections shown in Fig. 7D only tell a part of the story. SI must nucleate at a point, perhaps adjacent to a spreading ridge, then propagate along the weakness at plate tectonic rates (perhaps on the order of 100 mm/yr; Fig. 8G). The implied three-dimensionality of the Stern and Bloomer (1992) SI sequence implies that, in general a lithospheric weakness must be a few thousand km long to allow the lithosphere to sag sufficiently to ultimately fail and generate an IBM-style SI sequence. This predicts a certain scale to the products of SI events; they cannot be local features.

Recent confirmation and refinement of the Stern and Bloomer (1992) model comes from results of 2014 drilling by the International Ocean Discovery Program in the IBM system. IODP Expedition 352 (Fig. 6A) drilled into the Bonin forearc at four places, finding Eocene boninites in shallower water away from the trench and FAB in deeper water closer to the trench (Reagan et al., in press). These results indicate that the basalts erupted immediately after IBM SI have compositions similar to those generated by rapid sea-floor spreading at mid-ocean ridges, with little-to-no slab input. Subsequent melting to generate boninites involved more depleted mantle, and hotter and deeper subducted components, as subduction progressed and volcanism migrated away from the trench. Reagan et al. (in press) concluded that the volcanic sequence sampled during IODP 352 is akin to that recorded by many ophiolites, supporting a direct link between subduction initiation, fore-arc spreading and ophiolite genesis. This volcanic sequence sampled during IODP 352, with tholeiites overlain by boninites, is consistent with that expounded in the “Subduction Initiation Rule” (SIR; Whattam and Stern, 2011). SIR explains the common ophiolitic association of boninites and other arc-like volcanic sequences with tholeiites as indicating formation in a proto-forearc during SI (Fig. 9).

The biggest surprise in recent studies of IBM SI came from IODP Expedition 351, drilled west of the Kyushu-Palau Ridge (U1438, Fig. 10A, C). This site targeted oceanic crust beneath ~1.5 km thick sediments thought to have been produced before Early Eocene SI, perhaps in Cretaceous time. IODP 351 drilled 150 m into the volcanic section of the buried crust and concluded on the basis of age constraints, petrology and geochemical characteristics that this crust is remarkably similar to IBM FAB, of similar composition and formed at the same time as that in what is now the forearc. Arculus et al. (2015) concluded that IBM SI magmatic activity was not limited to the present forearc; that the width of the zone affected by SI was much greater than heretofore appreciated; and that the magmatic fluxes associated with IBM SI were much greater than previously thought. It may be that the great width of SI-related magmatism and extension is responsible for the observation that the Kyushu-Palau Ridge – which is taken to mark the trace of the transform fault that collapsed to start IBM subduction – does not approximate a small circle around a paleo-Euler pole, as expected for a transform fault (Fig. 10A; Taylor and Goodliffe, 2004). Upper plate extension accompanying SI may have affected a broad region, including areas now west of the Kyushu-Palau Ridge, and distorted its original trend.

Another important constraint comes from geochronology; it seems that the sequence shown in Fig. 7D takes 6–8 Ma to accomplish, from first FAB eruption to establishment of a normal magmatic arc, ~100 km above the subducting slab (Ishizuka et al., 2011). It likely takes a similar amount of time for the sequence to propagate along the lithospheric weakness away from the point of SI nucleation (Fig. 8G). Some of the recent spontaneous subduction initiation models (Fig. 11) also suggest comparably rapid (6–10 Ma) timescales of the SI processes (e.g., Gerya et al., 2008; Nikolaeva et al., 2008; Dymkova and Gerya, 2013; Zhou et al., 2016), although further modeling effort is needed to better understand incipient subduction dynamics and magmatic evolution as well as natural signatures characteristic for spontaneous vs. induced SI scenarios.

6.3. Recent concepts and examples

In recent years, subduction initiation concepts and examples have become more diverse and elaborate (e.g., reviews by Stern, 2004; Gerya, 2011 and references therein). The importance of subduction initiation for maintaining plate tectonics (e.g., Gurnis et al., 2004; Stern, 2004; Ulvrova et al., 2017) as well as for initiating this regime on Earth (e.g., Bercovici and Ricard, 2014; Rey et al., 2014; Gerya et al., 2015) has been broadly recognized by Earth scientists. Without giving a complete overview of these developments, below we show three representative examples of recent cross-disciplinary studies elaborating on different induced and spontaneous SI mechanisms.

6.3.1. Induced SI at a preexisting fault: the Puysegur example

An interesting example of induced SI (Fig. 4) is found at the Puysegur convergent margin (Fig. 12A). This remarkably narrow subduction zone is found SSW of S. Island, New Zealand where a restraining bend affects the dextral Alpine transform fault. Highly oblique convergence at a rate of 35 mm/yr is partitioned between oblique subduction of the Indo-Australian plate eastwards beneath the Pacific plate at the Puysegur trench, thrusting within the trench slope, strike-slip faulting on the Puysegur Bank, and minor shortening within the Solander Basin (Fig. 12B, C). Subduction began ~11 Ma ago and something like a mini-volcanic arc has formed, represented by a single volcano (Melhuish et al., 1999). Solander volcano erupts adakitic andesite (Fig. 12D; Reay and Parkinson, 1997), which probably reflects slab melting. The Puysegur example contrasts with IBM SI in several ways: 1) Puysegur is a narrow convergent margin, only ~150 km wide, from 47°30′S to 46°S, whereas IBM is 2500 km long; 2) Puysegur SI was

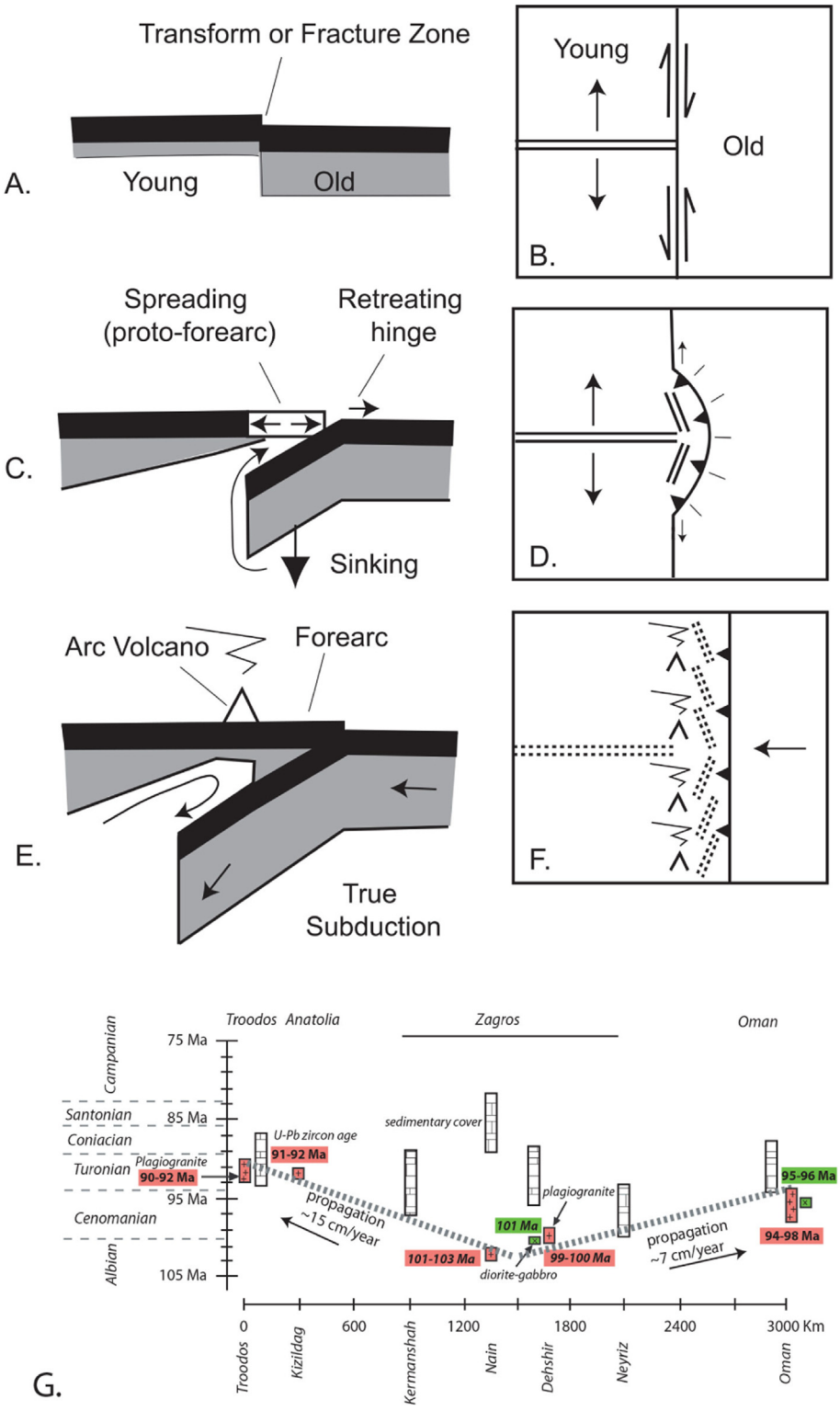

Fig. 8. Subduction infancy model of Stern and Bloomer (1992) modified to show the third dimension. Left panels are sections perpendicular to the plate boundary (parallel to spreading ridge) and right panels are map views. (A) and (B) show the initial configuration. Two lithospheres of differing density are juxtaposed across a transform fault or fracture zone. (C, D) Old, dense lithosphere sinks asymmetrically, with maximum subsidence nearest the fault. Asthenosphere migrates over the sinking lithosphere and propagates in directions that are both orthogonal to the original trend of the transform/fracture zone as well as in both directions parallel to it. Strong extension in the region above the sinking lithosphere is accommodated by seafloor spreading, forming infant arc crust of the proto-forearc. (E, F) The beginning of down-dip motion of the sinking lithosphere marks the start of true subduction. Strong extension above the sunken lithosphere ends, which also stops the advection of asthenosphere into this region, allowing it to cool and become forearc lithosphere. The locus of igneous activity retreats to the region where asthenospheric advection continues, forming a magmatic arc. (G) Compilation of U–Pb zircon dating results for Late Cretaceous Neotethyan subduction-initiation ophiolites along the 3000 km long Bitlis–Zagros ophiolite belt, after Moghadam et al. (2013). Biostratigraphic ages indicate the oldest reliable age for sediments either within or stratigraphically overlying the ophiolites. Note SI propagation rate ~100 mm/y.

induced (INSZ, Fig. 1) by change in Indo-Australian plate motions whereas IBM SI may have been spontaneous (spontaneous nucleation of subduction zone; SNSZ, Fig. 4); 3) Puysegur SI was accompanied by early compression and uplift (House et al., 2002); and 4) in contrast to early voluminous igneous activity for IBM, there is no evidence of forearc extension and volcanism for Puysegur SI.

Puysegur provides an excellent example of SI as a result of convergence across a pre-existing fault (Toth and Gurnis, 1998; Lebrun et al., 2003). What we don't know is whether or not a similar mechanism of forced convergence can produce a new convergent margin on the much larger scale of the IBM convergent margin (~2500 km vs ~150 km). The Puysegur example suggests that it is not easy to propagate SI along strike in this system; SI began ~11 Ma and has not propagated significantly since that time (House et al., 2002).

6.3.2. *Induced SI at a mid-ocean ridge: the Oman example*

A well documented possible example of a "fossil" SI by mid-ocean ridge inversion is represented by the Oman ophiolite complex (e.g.,

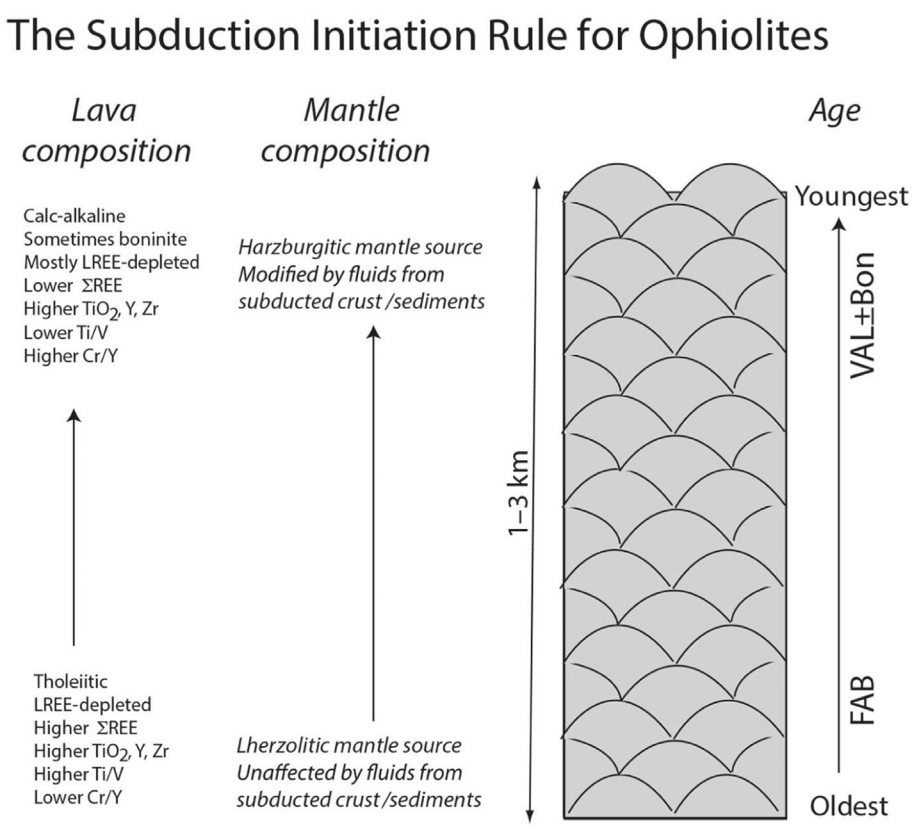

Fig. 9. The subduction initiation rule for ophiolitic volcanic successions (modified after Whattam and Stern, 2011; Stern et al., 2012). The crust of forearcs usually form as a result of subduction initiation and preserve systematic variations in basalt compositions (left) from MORB-like at the base to boninitic or arc-like at the top. This reflects changes in the source mantle as a new subduction zone starts, beginning with adiabatic upwelling of unmodified asthenosphere to form MORB-like "Forearc Basalts" (FAB) by seafloor spreading. Fluids from the sinking lithosphere eventually reach and metasomatically re-enrich the increasingly depleted mantle source of melts. Asthenospheric upwelling diminishes with time and is ultimately replaced by induced convection as sinking lithosphere begins downdip motion (true subduction). This cools and isolates the mantle beneath the forearc, leading to establishment of a magmatic arc behind a cold, dead forearc. LREE: light Rare Earth Element; ΣREE: total REE concentrations; VAL: volcanic arc lava; BON: boninite.

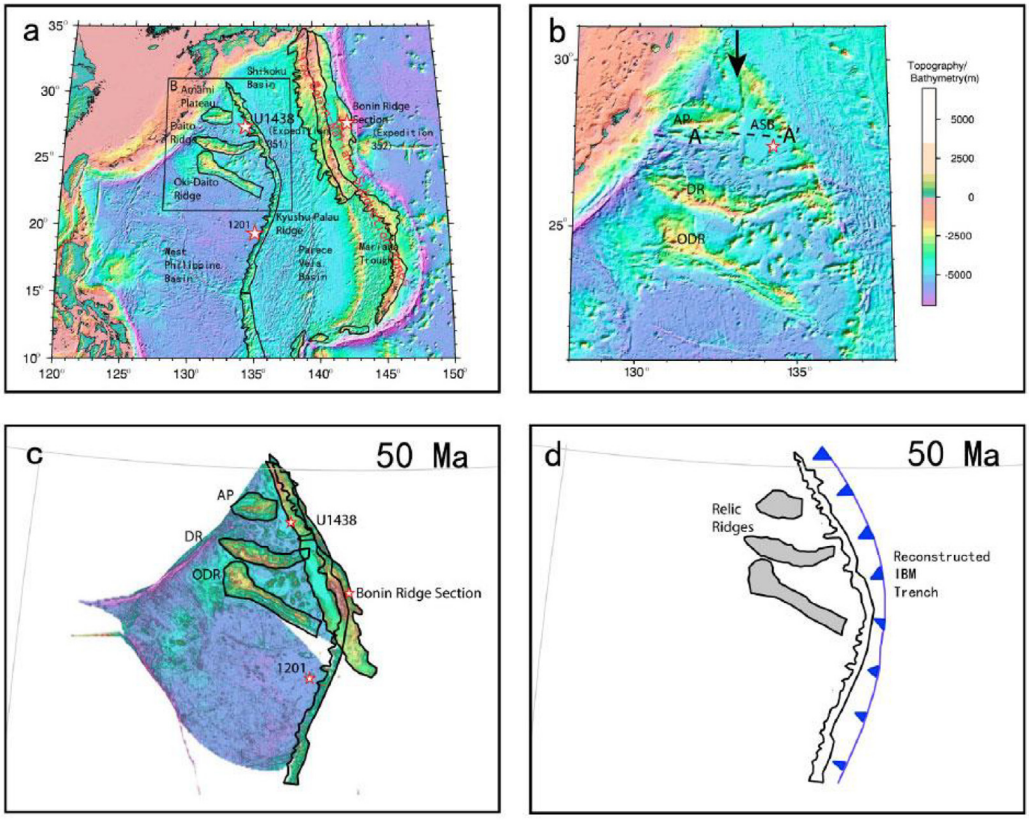

Fig. 10. Map view of IBM SI explored by Leng and Gurnis (2015). A) basemap of the Philippine Sea Plate showing the geometry at the time of IBM subduction initiation. b) Zoom in of the region drilled during IODP Expedition 351 (U1438) and 352, also drillsite shown by stars, the ASB (Amami Sankaku Basin) and three relic ridges: AP (Amami Plateau), DR (Saito Ridge), and ODR (Oki-Daito Ridge). The black arrow locates the presumed transform fault or fracture zone along which subduction initiation occurred. c) Reconstruction at 50 Ma of the present-day topography. d) Outlines of the relic arcs (in grey) indicating the location of the new trench (in blue) at 50 Ma. (For interpretation of the references to color in this figure legend, the reader is referred to the web version of this article.)

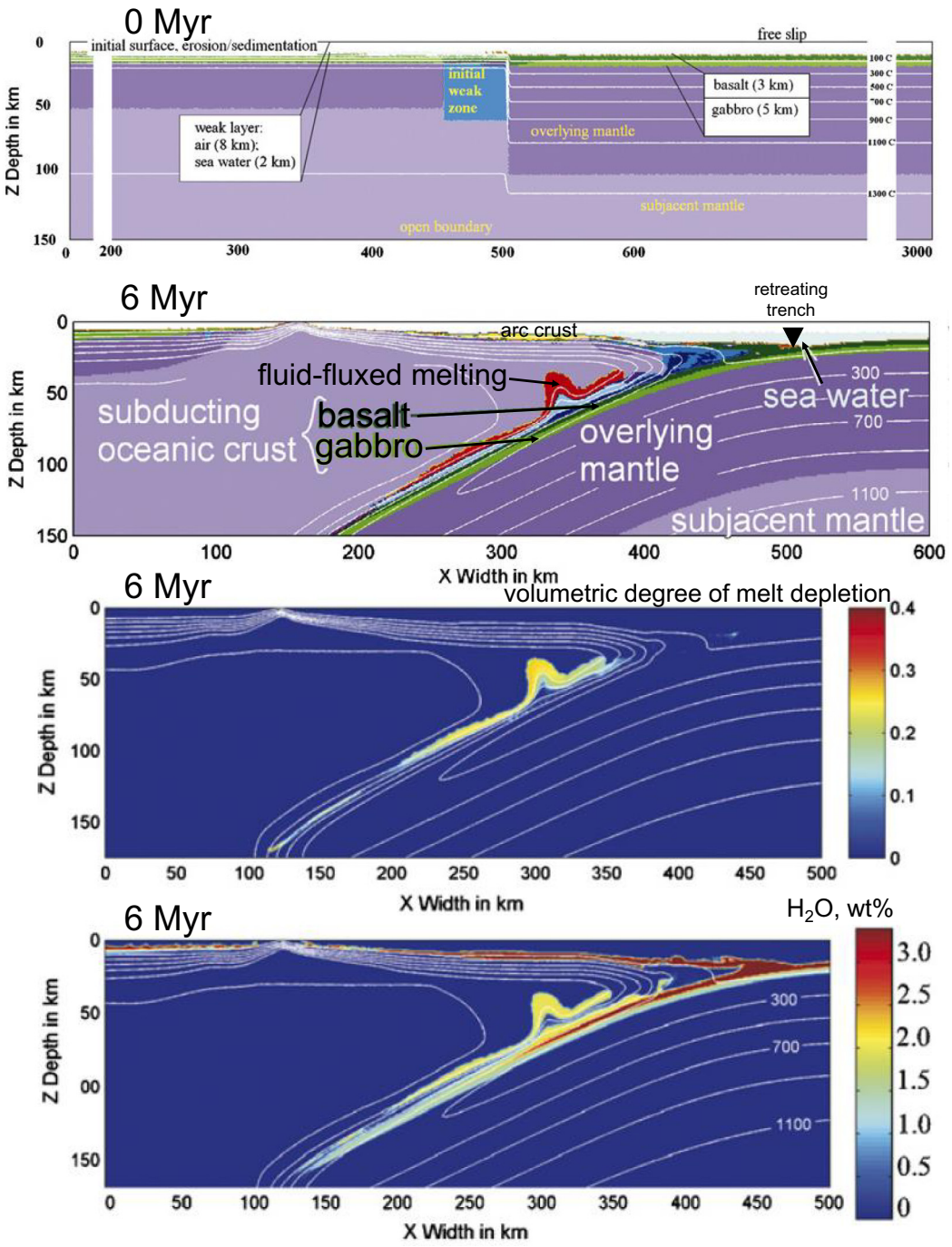

Fig. 11. Results of numerical experiments for spontaneous subduction initiation by transform collapse (Nikolaeva et al., 2008). By 6 Myr, a young oceanic plate with a backarc spreading center form as the result of the trench retreat. Young arc crust is formed by shallow fluid-fluxed mantle melting atop the retreating slab.

Agard et al., 2007, 2016; Duretz et al., 2016 and references therein). Obduction is an enigmatic process that emplaces large fragments of dense, oceanic lithosphere (ophiolites) atop continental crust and is directly linked to subduction initiation (Wakabayashi and Dilek, 2003). Among large-scale ophiolite exposures found worldwide (Oman, Turkey, Newfoundland, New Caledonia, and Papua New Guinea) (Monié and Agard, 2009 and references therein; Cluzel et al., 2001; Lus et al., 2004; Pubellier et al., 2004), the Oman case is particularly well documented and related to the infancy of subduction (e.g., Agard et al., 2007, 2016). The following first order geological-petrological constraints from the Oman region (Fig. 13A–C) are critical for subduction/obduction initiation models (Duretz et al., 2016 and references therein):

(1) *Final morphology of the ophiolite*: Emplaced ophiolite is represented by ~150–200 km long sequence up to 15 km thick (Fig. 13B and C).

(2) *Nappe stacking and reconstitution of the Arabian margin*: Ophiolite emplacement involved stacking of several nappes structurally delimited by tectonic contacts (Fig. 1B and C).

(3) *Syn-obduction sedimentation*: The maximum thickness of *syn*-obduction, foreland sediments reaches 1–3.5 km.

(4) *P–T–time paths*: Petrological data indicate a HP–LT metamorphic dome and a HT metamorphic sole found beneath the ophiolite, which are characterized by distinct burial and exhumation histories (Fig. 1D).

Based on these constraints, Duretz et al. (2016) investigated a series of two-dimensional (2D) thermo-mechanical models of compression-induced subduction initiation at a mid-ocean ridge followed by

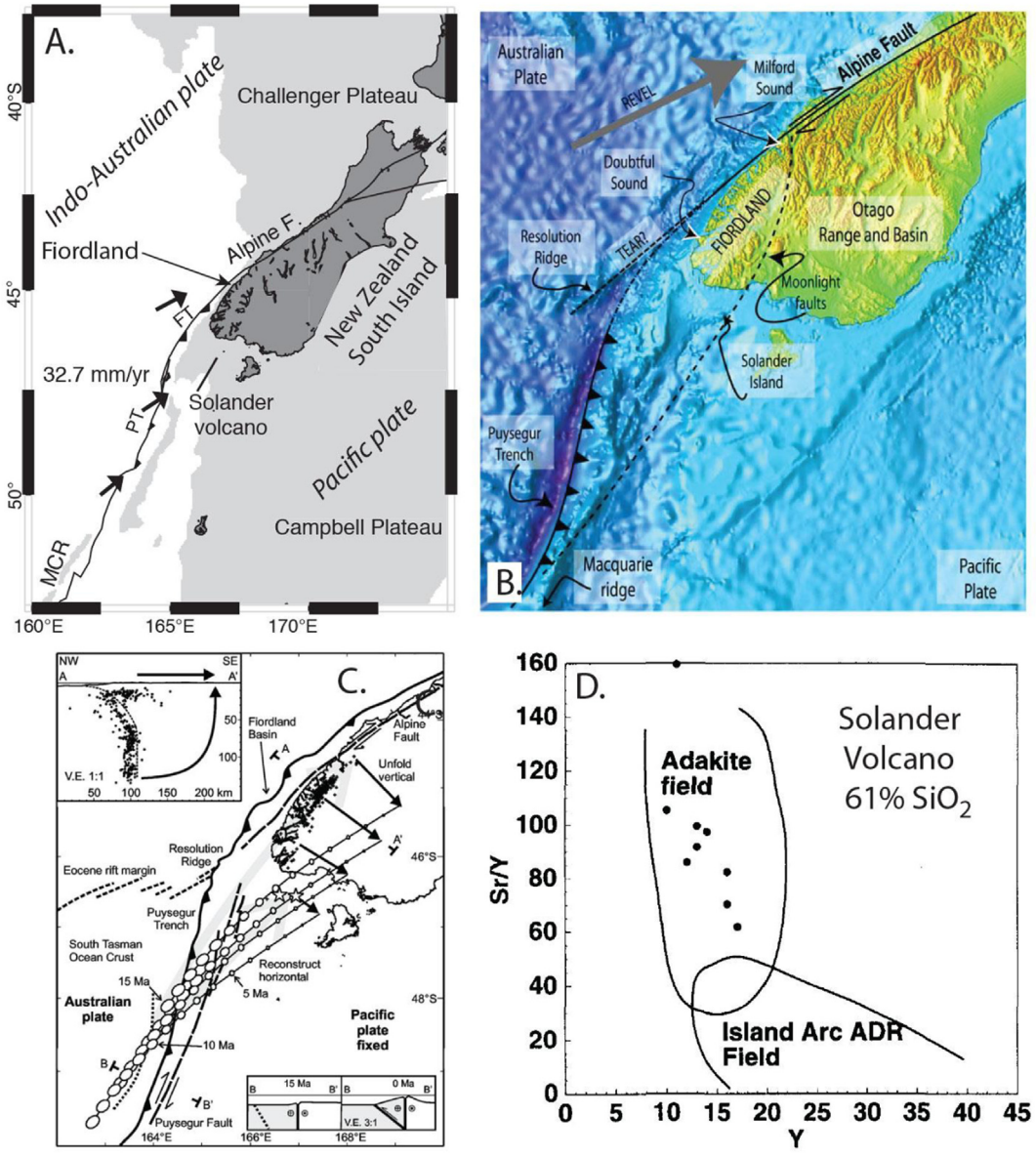

Fig. 12. The Puysegur transform and subduction zone, SW of New Zealand. A) Pacific-Australian plate boundary in S. Island New Zealand and submarine regions to the south. MRC = Macquarie Ridge Complex; FT = Fiordland Trench. Arrows show Indo-Australian plate motion relative to Pacific plate based on NUVEL-1A (33 mm/y); the plate boundary to the N and S of Puysegur region is a right-lateral transform fault (including the Alpine fault). Teeth show where new subduction zone has formed. Uplift in Fiordland is a result of forced convergence to form the Puysegur subduction zone Modified after House et al. (2002). B) Topo-bathymetry map of the southwestern corner of the region. The map includes the geographic references used in the text. Present day Au/Pa plate motion from REVEL. C) Unfolding and reconstruction of the Puysegur-Fiordland subduction zone. Crosses on the maps are earthquake epicenters > 50 km deep. Crosses on section A-A′ are earthquake hypocenters within 40 km of section A-A′ project along azimuth 040°. Stars show the location of young volcanic features, ~70 km above top of subducted slab. Bold arrows represent the effect of unfolding the subducted plate, so that it is restored to the Earth's surface with its down-dip line length preserved. The trajectory of sequential ellipses is the reconstruction of that point interpolated at m.y. increments. Each ellipse is a 95% confidence for locations. Large grey arrows are surface projection of the inferred trajectory of points on the deepest part of the subducted slab. Bold long-dashed lines are dextral strike-slip faults. The active subduction thrust trace is ornamented with teeth. Its initial position (Pacific plate reference frame) before 50% shortening west of the Puysegur Fault is inferred with a bold dotted line. Section B-B′ shows the inferred scenario that the Puysegur Ridge plate boundary evolved from an active transform fault to a partitioned oblique-subduction zone by capture of the Australian plate (Sutherland et al. 2006). D) Sr/Y vs. Sr diagram to illustrate adakitic affinities of Solander volcanics, from Reay and Parkinson (1997). Adakite may reflect slab melting as opposed the normal arc andesite-dacite-rhyolite (ADR) suites, which reflect low P fractionation of mafic melts.

lithospheric extension (Fig. 13E). The model reproduces SI away from the Arabian margin followed by the emplacement of the Oman ophiolite on top of it, culminating in lithospheric extension associated with domal exhumation of the metamorphosed margin through the ophiolitic nappe. A systematic parametric study indicated that 350–400 km of initial shortening fits both maximum pressure–temperature conditions of the metamorphosed margin (1.5–2.5 GPa/450–600 °C) and the dimension of the ophiolitic nappe (~170 km width). An important result of this study is that a thermal anomaly (e.g., mid-ocean ridge) located close (~100 km) to the Arabian margin is critical for obduction after subduction initiation (Duretz et al., 2016).

Geological-petrological data from the Oman region also suggest a distinct structural-lithological evolution of infant subduction zones (Agard et al., 2016), when slabs start to descend into the mantle. This stage coincides with the transient (yet systematic) transfer of material from the top of the slab to the upper plate, as witnessed by metamorphic soles welded beneath obducted ophiolites (Fig. 13). Agard et al. (2016) suggested that two successive rheological switches could exist across the incipient subduction interface due to mantle wedge serpentinization (mantle wedge vs. basalts, then mantle wedge vs.

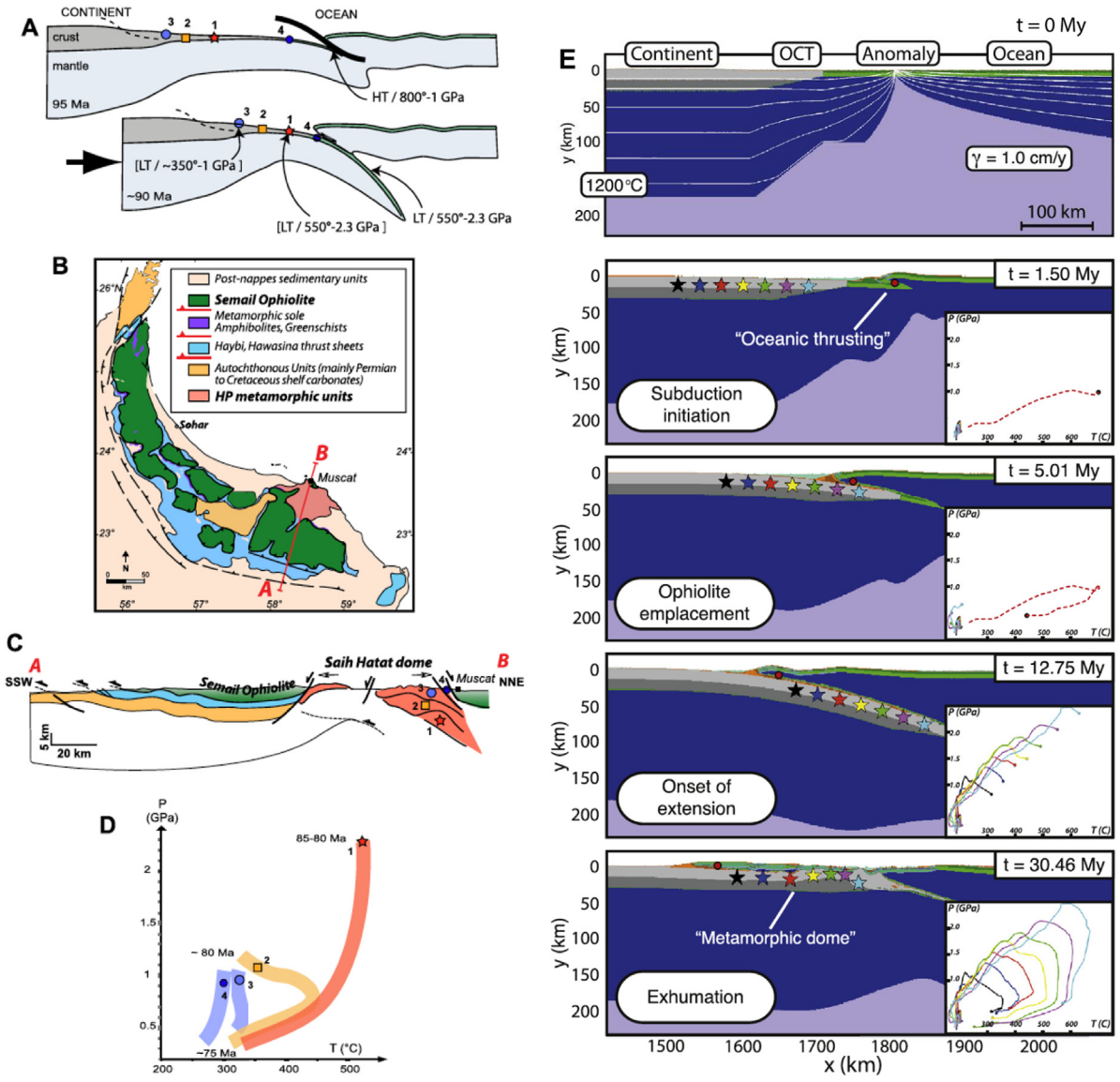

Fig. 13. Geodynamic concept (A), geological data (B), (C), P-T paths (D) and the numerical subduction/obduction initiation model (E) for the Oman ophiolite (Duretz et al., 2016). (A) Conceptual model of emplacement of oceanic units atop the continental margin. (B) Simplified geological map highlighting the dimensions of the ophiolitic nappe and the location of high pressure (HP) units. (C) Interpretative cross section through the ophiolite and the metamorphic dome of Muscat (filled square, white square, white star and black star indicate the continental units of decreasing metamorphic grade). (D) Compilation of P-T and geochronological data related to the continental margin metamorphism (the four pressure–temperature paths correspond to the symbols used in the above panels). (E) Temporal evolution of the model starting from intra-oceanic subduction induced by the ridge shortening to the domal exhumation of continental material beneath the overlying ophiolite. The colored stars denote the material points used to trace the P-T evolution in the continental margin. The red dot corresponds to a tracer located in the oceanic crust, whose P-T evolution is represented by the red dashed line. (For interpretation of the references to color in this figure legend, the reader is referred to the web version of this article.)

sediments; at ~800 °C and ~600 °C, respectively). These switches may control accretion of respective crustal rock rheologies, thus producing a distinct lithological structure of obducted ophiolite sequences (Fig. 13B). Transfer of material from the lower to the upper plate is also consistent with numerical modeling results (Fig. 13E) and may also be characteristic for spontaneous oceanic subduction initiation (e.g., Dymkova and Gerya, 2013).

It should be mentioned that the concept of induced subduction initiation at MOR is controversial and needs further studies. Recently, Maffione et al. (2017) presented new paleospreading directions from six Late Cretaceous ophiolites of Turkey, Cyprus, and Syria. They showed that ~NNE-SSW subduction zones formed within the Neo-Tethys during the Late Cretaceous, which they proposed were part of a major step-shaped subduction system composed of ~NNE-SSW and ~WNW-ESE segments. Maffione et al. (2017) inferred that this subduction system developed within old (Triassic?) lithosphere, along fracture zones and perpendicular weakness zones. It should also be noted that MOR lithosphere is buoyant, so it is important to understand whether or not compression of such lithosphere can lead to sustainable subduction. Obduction driving forces and dynamics also need to be better understood from both natural observations and numerical modeling perspectives. In particular, the Semail ophiolite is the eastern end of an ~3000 km Late Cretaceous ophiolite belt that can be traced from Oman through Iran, Iraq, Turkey, and Syria to Cyprus (Fig. 8G), and the origin of this ophiolite belt must be considered together, not in isolation. The alternative explanation — that Late Cretaceous SI on the SW margin of Eurasia was caused by SNSZ transform margin collapse (Moghadam et al., 2013) should also be considered. The transform margin collapse model (as well as any other SI model applied to this region) should however be tested numerically with both paleomagnetic data (e.g., Maffione et al., 2017) and *P-T-time* paths of metamorphic soles (e.g., Agard et al., 2007, 2016; Duretz et al., 2016).

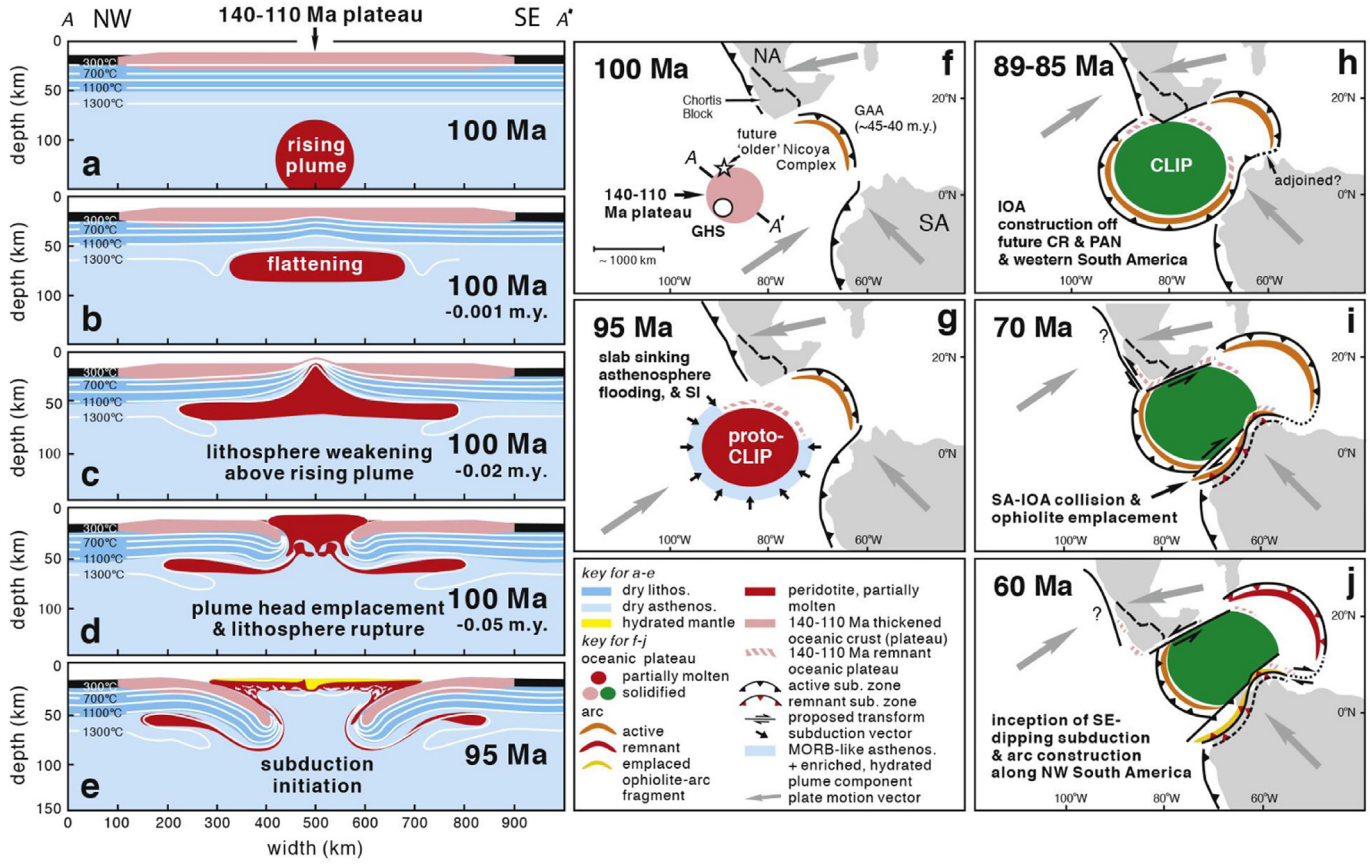

Fig. 14. Plume Initiated Subduction Initiation (PISI) model (a–e) and 100–60 Ma tectonic reconstructions (f–j). PISI model is modified from Ueda et al. (2008) and Burov and Cloetingh (2010). A (west) and A′ (east) for (a–e) is shown in (f). In (a), the (b) plume rises to the lithosphere base and flattens. (c) A central plume wedge rises and weakens the surrounding lithosphere. (d) The partially molten plume head ruptures the lithosphere and begins to spread above sinking oceanic lithosphere. (e) Subduction initiates in response to plume emplacement. (f) The Farallon Plate comprised a segment of circa 140–100 Ma thickened oceanic crust represented at least in part, by the 140–110 Ma segment of the Nicoya Complex, western Costa Rica (see text); this older thickened oceanic crust was likely the substrate upon which the < 100 Ma CLIP was constructed. As depicted in (a–e), emplacement of the mantle plume head above the Galapagos hotspot (GHS) (f) instigates (g) lithosphere sinking, subsequent asthenospheric flooding and ultimately SI. (h) SI results in arc construction along Costa Rica and Panama, western South America in Ecuador and Colombia and the Leeward Antilles (Aruba and Curaçao) (PISI traces 1–3, Fig. 1). (i) Collision of South America with the arc system off of western South America at ~70 Ma results in emplacement of intra-oceanic arc (IOA) ophiolitic fragments (dark yellow) in Colombia and Ecuador. (j) E/SE dipping subduction nucleates to the west of South America. (For interpretation of the references to color in this figure legend, the reader is referred to the web version of this article.)

6.3.3. *Spontaneous plume-induced SI: the Caribbean example*

Recently it has been proposed that a sufficiently long-lived, hot, and spatially extensive plume head can rupture the lithosphere and cause SI. This rather provocative suggestion was first made by Ueda et al. (2008) who carried out 2D numerical experiments and showed that in some cases a mantle plume can weaken the lithosphere above it sufficiently to initiate self-sustaining subduction (Fig. 14A–E). Ueda et al. (2008) demonstrated that lithospheric weakening reflects the plume volume, plume buoyancy, and the thickness of the lithosphere and is the greatest for the least buoyant purely thermal plumes. Burov and Cloetingh (2010) built on these promising results by carrying out 2D numerical experiments, confirming that SI was possible if a sufficiently buoyant plume head was emplaced beneath rheologically stratified crust and lithospheric mantle. The plume head flexes the lithosphere upward, exerts basal shears on it, and imposes local extensional stresses, at the same time heating it. The plume head erodes the mantle lithosphere and intrudes between buoyant crust and dense mantle lithosphere, allowing the lithosphere to sink and become a self-sustaining subduction zone. They also concluded that the size of the plume head was critical, that small plume heads could not cause SI

These ideas were intriguing, but the absence of a plausible natural example impeded serious consideration. This changed when Whattam and Stern (2015) made a strong argument that “plume-induced subduction initiation” (PISI) happened in Late Cretaceous time to form subduction zones around the S and W Caribbean plate. These formed in response to emplacement of an unusually large, hot, and long-lived plume, which was responsible for the ~100 Ma Caribbean Large Igneous Province (CLIP). Three key observations led to this conclusion: (1) Trace element chemistry of most 100 Ma and younger units interpreted as CLIP that are exposed along the southern margin of the Caribbean plate and NW South America, record subduction additions which increased with time beginning at 100 Ma; (2) There is no known hiatus between CLIP and younger arc lava sequences, suggesting continuous magma source evolution from plume to arc. (3) Generation of the CLIP and earliest, overlying and crosscutting arc units overlaps in time, space, chemical and isotopic compositions; both units are consistent with derivation from Galapagos plume-like mantle which became increasingly subduction-modified with time. These observations illustrate that formation of the CLIP and earliest arc volcanism reflects partial melting of the same hybrid plume-subduction-modified source. Whattam and Stern (2015) noted that the scale of the Caribbean PISI event was consistent with the expected large scale of the process, affecting the plume margins along two great arms some 1400 km from southern Costa Rica–Panama to western Colombia and 1700 km from Ecuador to the Leeward Antilles (Aruba and Curaçao).

The PISI model was tested by 3D numerical thermomechanical modeling by Gerya et al. (2015) to demonstrate that three key physical factors combined to trigger self-sustained subduction: (1) strong and negatively buoyant (i.e., sufficiently old) oceanic lithosphere; (2) focused magmatic weakening and thinning of lithosphere above the

plume; and (3) lubrication of the slab interface by hydrated crust. Details are shown in Fig. 16L–P. The numerical experiment showed that arrival of a sufficiently large, hot and long-lived mantle plume head could weaken strong and dense oceanic lithosphere to produce new self-sustaining subduction zones around the plume head, always dipping beneath the plume head, as seen for the present Caribbean.

6.4. Do passive continental margins collapse to form new subduction zones?

We close our historical overview of SI concepts and examples by discussing whether subduction initiates at passive margins. As noted in the Introduction, it is commonly assumed that, under certain circumstances, passive continental margins like those around the Atlantic Ocean, Gulf of Mexico, or western Indian Ocean, can transform to become new subduction zones. This is not only a critical aspect of the Wilson Cycle (as now articulated) but it is also reasonable from the perspective of lithospheric density and the additional load of thick sediments deposited on passive continental margins. However, distribution of the many new subduction zones that formed in Cenozoic and younger time does not include any examples that formed at a passive continental margin (with one possible exception, discussed below). This suggests that such an SI mode is difficult to accomplish. This difficulty may reflect the strength of old lithosphere that lies beneath passive continental margins, as first pointed out by Cloetingh et al. (1989). Cloetingh et al. (1989) considered in detail the strength problem and concluded that if a passive margin did not turn into a convergent margin in the first 20 Ma of its existence, the growing strength of the lithosphere beneath it made it increasingly unlikely to ever do so.

A number of works report evidence for compression at some passive continental margins, for example continentward dipping thrust faults offshore Argentina and Brazil, which Marques et al. (2013) interpret on the basis of 2D numerical thermomechanical models as representing an early “Brazilian Stage” SI triggered by a combination of several topographic loads with thin and warm continental margin lithosphere. This is characterized by ~10 km deep reverse fault seismicity at the margin, recent topographic uplift on the continental side, thick continental crust at the margin, and bulging on the oceanic side due to loading by the overthrusting continent. Self-sustaining subduction with arc igneous activity on the overriding plate has not yet developed, although its future occurrence after some millions years has been predicted by thermomechanical models (Nikolaeva et al., 2011; Marques et al., 2013).

Passive margins around the Iberian Peninsula provide three possible examples of SI at a passive continental margin. Along northern Iberia, opening of the Bay of Biscay led to shortening and formation of a marginal trench (Le Pichon and Sibuet, 1971). Alvarez-Marron et al. (1997) noted that oblique convergence of France and Iberia beginning in Early Cretaceous time produced the Pyrenees collisional orogen in the east and forced Bay of Biscay oceanic crust beneath the North Iberian margin in the west. Offshore multichannel seismic profiling revealed continentward-dipping thrust faults and an accretionary prism, and Alvarez-Marron et al. (1997) concluded that about 35 km of oceanic lithosphere was underthrust northern Iberia in middle Eocene to early Miocene time. Ruiz et al. (2017) carried out seismic imaging of lithospheric structure in this region and documented the indentation of Bay of Biscay crust into the Iberian crust and call this arrested overthrusting “subduction”. West of Iberia, on the Galician margin, Boillot et al. (1978) recognized that Mesozoic extension was followed by Eocene compression, but no evidence of sustainable subduction is found. We can thus summarize that there is evidence of compression and overthrusting in N. and W. Iberia, but self-sustaining subduction with arc igneous activity on the overriding plate never developed. This may be explained by local continental margin properties (e.g., lithospheric density and thickness, Moho temperature), which enable overthrusting but not subduction initiation (Nikolaeva et al., 2010, 2011).

The most interesting example of a passive margin that might have transformed into a subduction zone is found offshore SW Iberia and NW Africa, west of the Alboran Sea and the Straits of Gibraltar, in a region of complex tectonics known as the Gibraltar Arc (Gutscher et al., 2012). This lies along the complex plate boundary between Africa and Eurasia that marks the offshore part of the tightest and smallest orocline on Earth, the Betic-Rif arc, which changes in trend through 180° and has a radius of curvature of ~100 km (Platt et al., 2013). Evidence that surface materials were taken 50 km deep or more and returned to the surface are preserved as metamorphic complexes in Spain and Morocco. The purported subduction zone is quite narrow, about 200 km from N to S. There is seismicity down to ~140 km depth but this clusters and does not clearly define a Wadati-Benioff Zone (Thiebot and Gutscher, 2006). E-W tomographic sections across the region reveal a fast Vp region that dips steeply eastward to vertical in the upper mantle (Gutscher et al. 2002); this could be an E-dipping slab of oceanic lithosphere.

Interpretation of the Gibraltar Arc as marking a subduction zone has been challenged by Platt et al. (2003), Marques (2010) and Platt et al. (2013). Platt et al. (2003) argued from Africa-Eurasia relative plate motions that a N-S plate boundary in this region would be divergent, not convergent. They outlined several other challenges to the idea that the Gibraltar arc is above a subduction zone and also re-interpreted tomographic images as indicating a lithospheric drip (Rayleigh-Taylor instability), not a subducted slab. Marques (2010) noted that the Gibraltar accretionary wedge is dissimilar to that expected from subduction. Platt et al. (2013) emphasized the complex tectonics of this region and outlined 4 different ways that the structures of the Betic-Rif-Gibraltar arc could have formed: A) lithospheric delamination, B) slab break-off; C) convective removal of lithosphere; and D) slab rollback (essentially Gutscher et al. model) Platt et al. (2013) summarized geodetic data showing that the Alboran region straddles the Africa and Eurasia plate boundary, which is experiencing 4–6 mm/yr of right-lateral shear.

It should be noted that the aforementioned conclusions were reached before we knew that there were two kinds of transitional crust beneath passive margins. Transitional crust is intermediate in nature between continental and oceanic crust and is difficult to study because it is submerged underwater beneath thick sediments. It has long been accepted that such crust is composed of stretched and faulted continental crust but we now also know that much transitional crust is produced by igneous activity at the time of continental break-up. The “Volcanic Rifted Margin” (VRM) paradigm is widely accepted today and perhaps ~90% of all passive continental margins may be VRMs (Menzies et al., 2002). The effects of these different types of transitional crust may exert minor controls on passive margin SI because lithospheric strength mostly resides in the cool upper mantle. There is no evidence that either type of passive margin is more or less likely to collapse into a subduction zone, neither seems to happen. The comment of Mueller and Phillips “Simple models of passive margin failure, despite their popularity, cannot be quantitatively substantiated and are not evident in the geologic record” is as true today as it was when they said it in 1991 (p. 662).

In spite of the relative scarcity of geologic evidence that passive margins collapse to form new subduction zones, geodynamicists continue to consider and model evolution of passive margins in both two and three dimensions in order to understand their potential for both spontaneous and induced subduction initiation (e.g., Turcotte et al., 1977; Faccenna et al., 1999; Regenauer-Lieb et al., 2001; Goren et al., 2008; Nikolaeva et al., 2010, 2011; Marques et al., 2013, 2014; Marques and Kaus, 2016). These studies often reveal that additional processes, such as hydrous plumes and/or rifting (Fig. 7E) are needed to weaken old continental margins and cause them to collapse (Kemp and Stevenson, 1996; Regenauer-Lieb et al., 2001; Van der Lee et al., 2008; Nikolaeva et al., 2010, 2011).

Turcotte et al. (1977) considered the evolution of passive (Atlantic-type) continental margins by investigating models for the free and

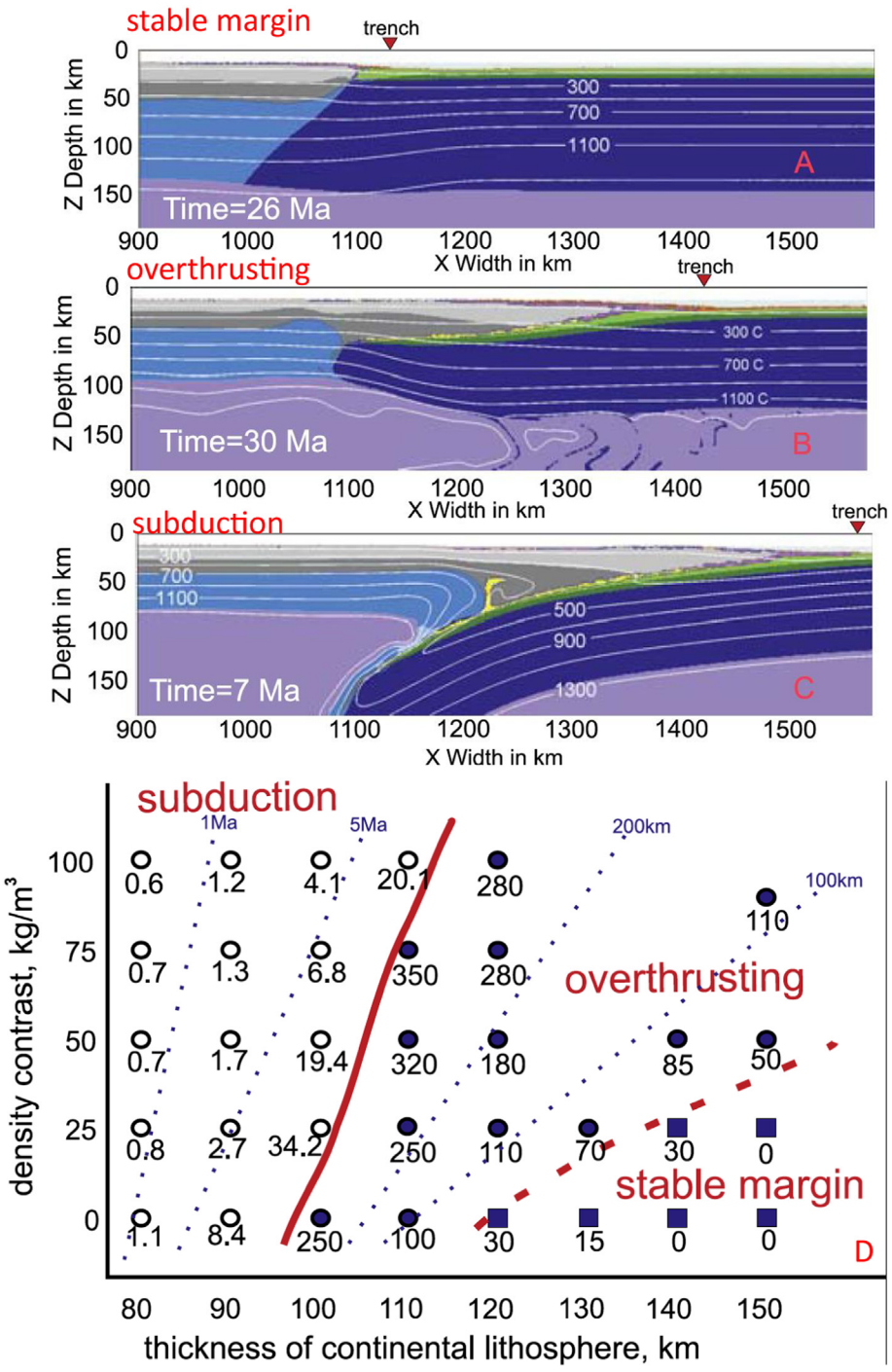

Fig. 15. Three different geodynamic regimes of passive continental margin evolution – stable margin (A), overthrusting (B) and subduction initiation (C) – formed in numerical experiments as a function of thickness of the continental margin and chemical density contrast between oceanic and continental lithospheres (D) (Nikolaeva et al., 2010).

locked flexure of the adjacent continental and oceanic lithosphere. They estimated that relatively large (several tens of MPa) lithospheric bending stresses should persist through the entire history of the margins. Based on observed gravity anomalies, they argued that the continental margin fault system must remain active throughout much of the evolution of the margin. The displacements along the faults should accommodate both the subsidence of the cooling and thickening oceanic lithosphere, and the sedimentary loading. It has been in particular suggested that this loading may be responsible for the seismicity on the eastern continental margin of the United States. Later, Regenauer-Lieb et al. (2001) investigated the process of sedimentary loading numerically and concluded that hydration-induced weakening of the bending oceanic lithosphere is needed to enable its large-scale faulting potentially leading to spontaneous subduction initiation.

Nikolaeva et al. (2010) investigated spontaneous SI at a passive margin numerically by analyzing factors controlling passive margins stability such as age of the oceanic plate, thickness of the continental lithosphere and crust, and density contrast between subcontinental and suboceanic lithospheric mantles. Results of systematic numerical experiments showed that three tectonic regimes can develop (Fig. 15): (1) stable margin (Fig. 15A), (2) overthrusting (Fig. 15B) and (3) subduction (Fig. 15C). It has also been demonstrated that whereas transition from stable margin to the overthrusting regime is mainly controlled by ductile strength of the lower continental crust, the transition from overthrusting to subduction regime is governed by the chemical buoyancy and ductile strength of the subcontinental lithosphere. In

contrast to McKenzie (1977) who investigated compressional brittle failure of the oceanic lithosphere, numerical models of Nikolaeva et al. (2010) suggested that passive margin collapse is driven by the ductile shearing of anomalously thin and warm continental margin lithosphere. The collapse starts by the buoyant overthrusting of the extending continental margin over the passively bending and retreating oceanic plate (Fig. 15C) (Goren et al., 2008; Nikolaeva et al., 2010; Marques et al., 2013, 2014). This spontaneous passive margin collapse is thus in contrast with induced subduction initiation investigated by Faccenna et al. (1999) using analogue models, which suggest underthrusting of the kinematically driven oceanic plate under the shortening continental margin. The age of the oceanic lithosphere does not play any significant role in the passive margin collapse (Nikolaeva et al., 2010), whereas main controlling factors are the continental Moho temperature and the chemical buoyancy of continental mantle (Fig. 15D). Experiments of Nikolaeva et al. (2010) clearly demonstrated that only anomalously thin and hot (Moho temperature $>$ 660 °C) continental margins could develop subduction (Fig. 15D) (Nikolaeva et al., 2010). In particular, the south Brazilian margin characterized by high heat flux, significant topographic loading and increased seismic activity has been identified as a potential area for SI whereas other American Atlantic margins remain stable (Nikolaeva et al., 2011; Marques et al., 2013).

Recently, Marques et al. (2014) investigated spontaneous SI at both straight and curved passive margins using 3D thermomechanical models. They found that the dynamics of SI is mainly controlled by the lateral pressure gradients, arising from density differences between oceanic and continental crust. The orientation of the pressure gradients in 3D depends on the margin curvature and in case of a curved margin can produce a horizontal, along-margin component of crustal and mantle flow. This flow partitioning can in turn impede the SI by slowing down slab bending and related increase in the effective slab pull. Marques et al. (2014) concluded, in particular, that the pronounced curvature in the southeast Brazilian margin is a likely explanation why subduction initiation is hampered there.

It might be thus worthwhile to consider that the absence of widely accepted modern examples of SI at passive margins is telling us about the high lithospheric strength of these regions, which precludes SI. On the other hand, numerical studies indicate that subduction initiation indicators at passive margins should be very different from these for mature subduction (e.g., Nikolaeva et al., 2010, 2011; Marques et al., 2013), which may create difficulties in discovering this process in nature. It should also be noted that an alternative mechanism of passive margin rejuvenation by STEP (subduction tear edge propagator) fault formation associated with convergent margins invading an ocean basin – for example the S. Scotia convergent margin that has recently migrated into the S. Atlantic – has been proposed and modeled numerically (e.g., Baes et al., 2011; Duarte et al., 2013; Chertova et al., 2014). Thus, the feasibility of passive margin collapse remains unresolved and more work is needed to reconcile concepts and modeling results with observations.

7. Modern approaches and results

7.1. SI in numerical models

Increasing computer processing power and improved understanding of rock rheology are leading to rapid improvements in our understanding of SI. Some examples of advances in geodynamic modeling of subduction initiation over the past 15 years are shown in Fig. 16. These examples are not intended to be exhaustive but they do capture important differences in approach, technique, and topics. The five studies that we discuss below and show in Fig. 16 explore 2D models of how induced and spontaneous SI proceed (respectively Hall et al., 2003; Gerya et al., 2008); 2D models of how magma compositions change as induced SI proceeds (Leng et al., 2012); 3D models of how mantle plumes can cause SI (Gerya et al. 2015); and 3D models of how SI affects and is affected by global mantle circulation and plumes (Crameri and Tackley, 2016).

Hall et al. (2003) used a 2D visco-elastoplastic model (200–300 km deep, 800–1000 km deep, with variable resolution) using the Fast Lagrangian Analysis of Continua (FLAC) method to show that a fracture zone could be converted into a self-sustaining subduction zone after approximately 100 km of convergence. They used a realistic non-linear, temperature-, pressure- and stress-dependent rheology to model induced SI within first 6.8 million years at a fracture zone with a 40 Myr age offset and imposed convergence of 2 cm/yr. Their modeling showed that even in the case of induced SI, the lithosphere would fall rapidly, drawing in asthenosphere needed to induce forearc spreading (Fig. 16A–D).[2]

Gerya et al. (2008) looked at the possibility that an oceanic fracture zone juxtaposing lithospheres of different age could spontaneously collapse to form a subduction zone. They constructed a 2D rectangular grid with 511 × 113 finite-difference points with a non-uniform spacing of 1–30 km (2 × 1 km to 2 × 2 km spacing around the weak zone) to model what happened in a box ~1000 km wide and ~200 km deep. Equations of conservation of momentum, mass, and energy were solved based on finite-differences and marker-in-cell technique; results are summarized in Fig. 16E–H. 71 numerical experiments systematically varied the presence or absence of water, rate of fluid migration, plate ages, size of the initial weak zone, and plastic strength of crustal and mantle rocks. Gerya et al. (2008) found that spontaneous SI depends on the size and strength of the initial weak zone; the larger and weaker, the better for SI. As SI begins, the rocks of the weak zone are sheared along the top of the sinking plate, creating a weak layer that lubricates plate movement. Subsequent development depends on the brittle/plastic strength of the plates and the presence of a weak hydrated layer above the descending slab. When the plates are strong and no weak hydrated layer is present atop the slab, subduction ceases after several million years as the interplate shear zone thins. Gerya et al. (2008) note that trench rollback occurred in all simulations, consistent with geologic constraints from IBM and ophiolites. The strong influence of fluid percolation on transform collapse has been recently confirmed by Dymkova and Gerya (2013) on the basis of coupled hydro-thermo-mechanical model of SI accounting for rock deformation enabled by percolation of fluids at the incipient subduction interface.

We are also beginning to quantitatively explore how magma generation evolves during SI. Leng et al. (2012) modified the 2D finite-element approach of Hall et al. (2003) with induced SI to which they added parameterized melting to determine the magmas produced in response to different SI modes (Fig. 9I–K). They used simplified major element compositions (8 major elements and reasonable approximation for initial mantle phase proportions (in weight percent): olivine 57%, orthopyroxene 28%, clinopyroxene 13%, and spinel 2%. Each time a particle moves to a new position, they computed the extent of melting from the temperature, pressure, water content, and weight percent of modal clinopyroxene. Leng et al. (2012) found that the foundering of the subducting slab and water release from the slab govern a succession from basalts with compositions similar to mid-ocean-ridge basalts (MORB) to boninites, as seen for the IBM forearc and ophiolites (Fig. 9). The modeled transition from MORB-like to boninite composition typically occurs within a few million years. When plate strength is reduced, the subducting slab tends to segment, with extensive melting occurring when the slab breaks; most melting occurs close to the trench. When plate strength increases, subduction initiation becomes continuous without infant-arc spreading; such a mode leads to a limited, very low degree of melting occurring during a long interval of plate convergence before SI starts, although extensive melting near the trench is still possible when subduction initiation starts after a protracted period of

[2] An animation of this sequence can be found at http://web.gps.caltech.edu/~gurnis/Movies/Science_Captions/subduction_initiation.html

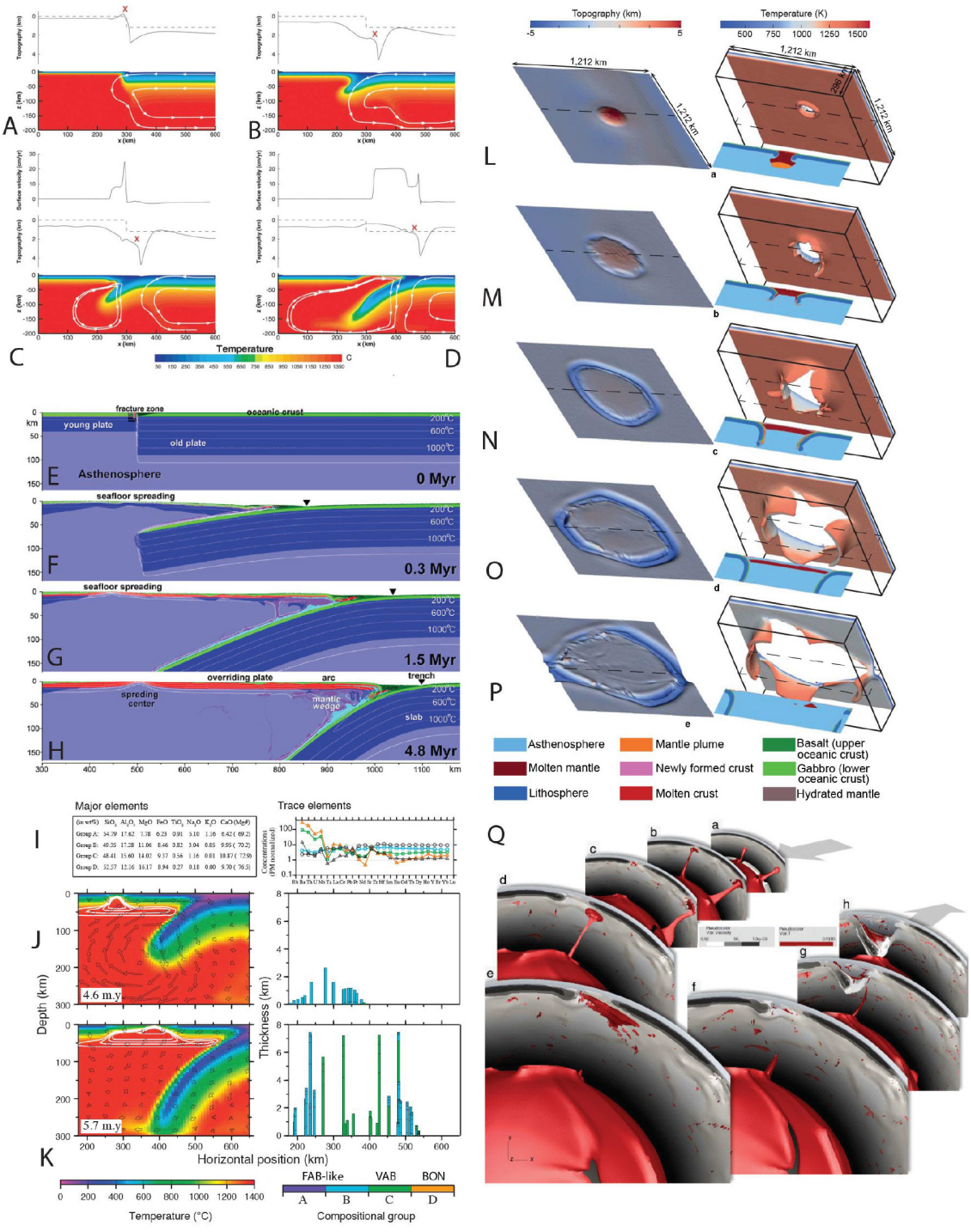

(caption on next page)

plate convergence (~10 m.y.). It would be interesting to see a similar study for magma generation and evolution accompanying spontaneous SI.

Gerya et al. (2015) conducted 3D numerical experiments of plume-induced SI (Fig. 16L–P). These numerical experiments took advantage of improved computing power and software development, which allowed design of a high-resolution tectono-magmatic plume-lithosphere interaction model that accounts for interaction between the plume and the oceanic lithosphere. The experimental design offers high numerical resolution (~3 × 3 × 2 km) based on optimized staggered grid/particle-in cell method. The tectono-magmatic interaction of the plume with the lithosphere was parameterized by monitoring melt extraction and upward transport from the plume, rheological weakening of the lithosphere subjected to melt percolation and crustal growth by both plutonic and volcanic additions. These experiments showed that melt-induced weakening of the lithosphere above the plume is critical for SI, which requires up to 100 times reduction of the effective brittle/plastic strength of the lithosphere penetrated by melts. Plume penetration and oceanic plateau growth induce significant lateral density contrasts at the plateau margins where lithosphere thickens by lateral convective flow removing weakened mantle rocks from the area atop the plume toward the plume margins. The instability reflects the juxtaposition of

Fig. 16. Some examples of advances in geodynamic modeling of subduction initiation, 2003–2016. A–D) 2D Model of Hall et al. (2003) for induced initiation of subduction at a fracture zone with a 40 Myr age offset and imposed convergence of 2 cm/year at four instances: A) 0.8 million years, B) 5.4 million years, C) 6.0 million years, and D) 6.8 million years. Each instance shows thermal structure, instantaneous flow lines (white), and current (solid) and initial (dashed) topography. The red 'x' shows the uplift and subsidence experienced by one unit of surface rocks. Panels C and D also show the horizontal component of surface velocity during the rapid extensional phase in the over-riding plate. E–I) Examples of numerical 2D models for spontaneous initiation of subduction at an oceanic fracture zone (Gerya et al., 2008). Note the much wider region affected by slab sinking in F than shown in Fig. 3D or 4C. Downdip motion begins in G, after only 1.5 million years of slab sinking. A mature subduction zone is established after ~5 Ma (H). I–K) Summary of petrogenetic modeling of magmas generated during forced SI (convergence of 4 cm/year; case A01) by Leng et al. (2012). Note that there will not be forearc extension, asthenospheric upwelling, or forearc spreading. I) Major element compositions and Mg# (= 100 × Mg / (Mg + Fe)) along with trace element patterns for 4 different types of SI-related magmas generated by progressive depletion and hydration of mantle source. J) Temperature, velocity, and melting extent contours at 4.6 M.y. K) the same model 5.7 M.y. after SI. Temperature scale and colors indicating compositional groups shown at the bottom. L–P) Dynamics of plume-induced subduction initiation under present-day mantle temperature conditions, from Gerya et al. (2015). Left side shows topography, right side shows subsurface structure. The plume head is implied, not shown for clarity. L) Oceanic plateau development (at 0.07 M.y. from the beginning of the experiment); M) formation of an incipient trench and a nearly circular slab (at 0.56 M.y.); N) tearing of the circular slab (at 3.79 M.y.); O) formation of retreating subduction zones (at 9.43 M.y.); and P), development of spreading ridges and transform boundaries (at 25.63 M.y.). Left and right columns show topography and subducted lithosphere morphology with projected slab surface temperature, respectively. Dashed lines indicate positions of the 2D cross-sections (color code is at the bottom of the figure). Q) Panels showing time snapshots of SI by global mantle flow. Temporal evolution of subduction initiation in a global, 3-D spherical experiment (*g l o b a l*4) showing the cold plates by viscosity isosurfaces (*grey*) and mantle plumes by a temperature isosurface (*red*). Individual snapshots highlight the different phases characterised by a. From onset of hot mantle plumes, b local lithospheric thinning, c–d development of strong LAB-topography through shallow horizontal mantle flow and an additional plume pulse, e–f plate failure, and finally g–h buoyancy-driven subduction (Crameri and Tackley, 2016). (For interpretation of the references to color in this figure legend, the reader is referred to the web version of this article.)

old, cold, dense (gravitationally unstable) oceanic lithosphere and young, warm, buoyant thinned lithosphere of the oceanic plateau, creating even greater gravitational instability that that triggering subduction along oceanic transform boundaries. Gerya et al. (2015) identified five stages of lithospheric collapse around the plume head leading to self-sustaining subduction; these can be subdivided into: (1) oceanic plateau formation by plume-induced magmatism (Fig. 16L); (2) formation of an incipient trench and a descending nearly-circular slab at the plateau margins (Fig. 16M). The oceanic plateau begins to collapse and flows radially outward over the surrounding colder oceanic plate, which gradually bends down and penetrates into the mantle thus forming an incipient nearly circular oceanic slab, while the plume head forms an embryonic hot mantle wedge atop the surrounding slab; (3) Slab descent is increasingly resisted by the ring confinement at the base of the encircling slab until it tears during deepening and rolling back under its own weight (Fig. 16N); (4) Slab tearing introduces asymmetry into the initially nearly-circular subduction system, splitting it into several independently retreating segments with different strikes and dip angles. This leads to the formation of several self-sustained subduction zones, each of which retreats from the expanding and flattening plume head (Fig. 16O). This is the stage when subduction becomes self-sustaining; and (5) cooling of the new plate formed between the retreating subduction zones and initiation of spreading centers and transform boundaries within this plate (Fig. 16P). Gerya et al. (2015) concluded that the critical parameter affecting feasibility of PISI is the intensity of magmatic weakening of lithosphere above the plume head, which controls the ability of the plume to penetrate the oceanic lithosphere and thus create the initial gravitational instability. Large, long-lived plume heads supplying hot mantle material to the bottom of the old, dense oceanic lithosphere favored PISI, small, short-lived, cool plumes did not favor PISI.

The above 4 numerical experiments looked only at a region that was a thousand kilometers wide and a few hundred kilometers deep. Crameri and Tackley (2016) looked at the effects of SI on global mantle circulation associated with breaking a stagnant lid — (Fig. 16Q). They carried out 2D and 3D numerical experiments using dynamically self-consistent, time-dependent numerical modeling of mantle convection with free upper surface condition. These experiments showed that mantle plumes impinging on the base of the plate weaken and thin it, at the same time producing topography on the lithosphere-asthenosphere boundary, which are critical for SI. Crameri and Tackley (2016) also found that plume-lithosphere interactions resulted in periodic global resurfacing and replacement of old lithosphere with new lithosphere, so that stagnant-lid silicate planets like Venus are likely to have short episodes of global overturn with multiple short-lived subduction zones rather than modern style terrestrial plate tectonics with long-lived subduction and a mosaic of plates (Bercovici and Ricard, 2014).

7.2. SI in laboratory experiments

Important new insights into rheological controls of SI processes are provided by laboratory experiments investigating rheological properties of hydrated crustal and mantle rocks (Escartín et al., 2001; Hilairet et al., 2007; Collettini et al., 2009; Carpenter et al., 2011; Amiguet et al., 2012; Hirauchi et al., 2016). These experiments demonstrated that localized weakening of the oceanic lithosphere in both brittle and ductile domain could be related to deformation-assisted hydration processes, which thus prepare favorable conditions for SI.

In particular, Escartín et al. (2001) investigated deformation of peridotite with 10–15% lizardite and chrysotile serpentine to determine the influence of serpentine content on the rock strength and the style of deformation. It has been demonstrated that the brittle strength of even slightly serpentinized peridotites is dramatically lowered, becoming comparable to that of pure serpentinite (friction coefficient = 0.15–0.45, Reinen, 2000; Reinen et al., 1994; Moore et al., 1996; Escartín et al., 1997). It has been shown that an abrupt transition from a "strong," peridotite rheology to a "weak," serpentinite rheology occurs at low degrees of serpentinization (10%–15% or less). It has also been suggested that weak serpentinized zones in the cooling oceanic lithosphere may form by deep water penetration associated with normal faulting at mid-ocean ridges (e.g., Escartín et al., 2001), thermal cracking of the lithosphere (Korenaga, 2007), and plate bending (Iyer et al., 2012).

Another important experiment investigated high-pressure (ductile) creep of serpentine and related it to the initiation of subduction (Hilairet et al., 2007). Low strength and viscosity of serpentine may strongly influence subduction-zone dynamics at all time scales, but until this work its role was not quantified experimentally. Deformation experiments on the serpentine antigorite at 1–4 GPa and 200–500 °C showed that the viscosity of serpentine is much lower than that of the major mantle-forming minerals. Moreover, due to the very low activation energy (ca. 10 kJ/mol), this low viscosity remains almost independent of temperature and can efficiently lower ductile strength of mantle lithosphere along hydrated faults. Such deeply penetrating hydrated structures can thus serve as favorable sites for future SI episodes. Later, Amiguet et al. (2012) explored the rheological behavior of polycrystalline lizardite, a serpentine group phyllosilicate that forms in oceanic and subduction contexts. High-pressure deformation experiments were carried out at 1–8 GPa and 150–400 °C. Experimental results and first-principles calculations confirmed easy gliding on lizardite basal planes and show that the flow stress of phyllosilicate is in the range of the critical value of 20–200 MPa down to depths of about 200 km. It has been concluded therefore that lithospheric weaknesses due to the presence of foliated serpentine or chlorite-bearing rocks are important for subduction initiation.

Hirauchi et al. (2016) showed experimentally that shear-enhanced

hydration reactions contribute to generating and maintaining weak mantle shear zones at mid-lithospheric depths, where the largest strength of the oceanic lithosphere resides (e.g., Bercovici and Ricard, 2014). Their high-pressure friction experiments at 1 GPa and 500 °C on peridotite gouge revealed that in the presence of water, increasing strain and reactions lead to an order-of-magnitude reduction in strength. It has been shown that the rate of deformation is controlled by pressure-solution-accommodated frictional sliding on weak hydrous phyllosilicate (talc), providing a mechanism for reducing strength at the brittle-plastic transition. Based on these experiments, Hirauchi et al. (2016) suggested that infiltration of seawater into long transform faults with low slip rates is an important controlling factor for SI and plate tectonics as suggested in many conceptual and numerical models (e.g., Stern, 2004; Gerya, 2011 and references therein).

Important experimental studies have also been conducted for understanding weak brittle-frictional properties of natural fault rocks (Collettini et al., 2009; Carpenter et al., 2011). Collettini et al. (2009) reported on the frictional strength of intact natural crustal fault rocks sheared in their in situ geometry. It has been found that samples with well-developed foliation are significantly weakened (friction coefficient = 0.25–0.31) compared to their powdered equivalents (friction coefficient = 0.43–0.55). Micro- and nanostructural studies showed that frictional sliding in these foliated rocks occurs along very fine-grained foliations composed of phyllosilicates (talc and smectite). Similar to the results of Escartín et al. (2001), Collettini et al. (2009) found that significant fault weakening occurred with a small percentage of weak minerals suggesting that low friction results from slip on a network of weak phyllosilicate-rich surfaces that define the rock fabric. Furthermore, Carpenter et al. (2011) showed that smectite-bearing fault rocks exhibit stable sliding friction behavior and show no frictional healing after rupture. Thus, mineralogically-controlled fault weakness are likely to be maintained in both space and time. Collettini et al. (2009) also noted that the abundance of foliated rocks along mature faults in different tectonic settings and from many different protoliths suggests that this mechanism could explain fault weakening in the brittle crust. This may lead to tectonic inheritance repeatedly proposed for SI (e.g., Bercovici and Ricard, 2014 and references therein).

8. The future

It is hard to predict where the rapidly-evolving field of SI will be over the next decade or two. It is likely that field studies and computational studies will increasingly inform each other and advance together, as was the case for the PISI breakthrough. A few lines of inquiry where significant progress is likely are outlined below.

8.1. Field and petrologic studies

Focused field studies about the timing and products of SI are needed. Certainly more studies of oceanic forearcs like IBM are called for, along with scientific drilling to recover intact sequences of SI products. It may be easier to carry these studies out on land, focusing on regions where a long ophiolite belt parallels a volcanic or plutonic magmatic arc. All ophiolites may not form during SI, but relatively intact ophiolite belts paralleling magmatic arcs are likely to represent fossil convergent margins, with the ophiolite belt marking forearc crust that formed when subduction began and the magmatic arc marking the locus of igneous activity that was established once true subduction began. Long (~1000 km) exposures of these belts are especially important to study; these can be found in California, Cuba, Iran-Anatolia, and S. Lhasa terrane, Tibet, and the Balkans. Focused geochronological studies promise to illuminate the rates at which SI proceeds at one location and the rates at which SI propagates along strike of the lithospheric weakness Another aspect of SI that could profitably be addressed from ophiolite studies is what is the distribution of MORB-like and arc-like (including boninitic) sequences in ophiolites? Are these mostly a vertical sequence (as argued by Whattam and Stern, 2011) or are there important lateral differences in distribution of these sequences? What do these distributions in space and time reveal about SI?

It would also be useful to address the passive margin collapse hypothesis via field studies. A concerted effort to find and document Cenozoic examples of this process – and to understand why passive continental margins do not produce sustainable subduction zones – would provide valuable constraints on geodynamic models.

8.2. Geodynamic modeling

Increased computational power is allowing numerical experiments to move from 2D to 3D modeling. Advances in 3D modeling are clearly going to drive SI science in the future, but there remain several areas where 2D studies can shed significant light. These include for example: 1) SI and magmagenesis; 2) SI and fluids; 3) why is polarity reversal easy and transference difficult? 4) what causes the transition between slab sinking and true subduction? and 5) why don't passive continental margins collapse into sustainable subduction zones?

For SI and magmagenesis, there is much to be learned. What are the links between SI and magmagenesis? Spontaneous SI requires a rapid reorganization of asthenospheric flow, from upwelling above the sinking slab at first to downwelling adjacent to the slab when true subduction begins. What if any link is there between the changing asthenospheric flow and changing magma compositions? Can we infer whether SI was induced or spontaneous from the distribution and composition of igneous rocks? For example, spontaneous SI will lead to forearc spreading such as for IBM but induced SI may not result in any igneous activity until the slab reaches ~100 km, as is seen for Puysegur.

In the case of spontaneous SI, we don't yet understand what causes the slab to transition from sinking to sliding down-dip to start true subduction. Is it because the sinking slab encounters more resistance from the underlying mantle? Does this resistance reflect just the progressively greater volumes of mantle that must move out of the way, or does it also reflect increasing viscosity of the mantle with depth into the asthenosphere and into the deeper parts of the upper mantle? What about changes in the slab itself, does the conversion of crust to dense eclogite play a significant role?

The conversion of passive continental margins into subduction zones is deeply embedded in the geoscientific subconscious, in spite of a lack of evidence that it happens. Why do these margins have so much strength? It may be more useful for the geodynamic community to examine in detail why passive margins are not sites of SI than to model how this might happen.

The increasing ability of geodynamic modelers to use realistic experimentally calibrated rheologies and forces to model SI in 3D is very exciting. This will allow us to investigate how SI starts at a single point along a lithospheric weakness and then propagates along that singularity. It will allow us to examine what if any limits there are to along-strike flexure of sinking lithosphere due to propagation of SI along a lithospheric weakness. Advances in 3D modeling will allow us to investigate likely modes of seafloor spreading in the forearc, and how magma compositions change along strike as SI propagates along the weakness. It will also allow us to examine how mantle flows above and below descending lithosphere as the latter changes along strike from sinking to subducting.

9. Conclusions

There are no firm conclusions to this progress report, but there are some preliminary ones. We are making good progress towards understanding how new subduction zones form by combining field studies to identify candidates and reconstruct their timing and magmatic evolution and undertaking numerical modeling (informed by rheological constraints) to test hypotheses. Even though we are in a computational

transition between 2D and 3D numerical modeling, we have good examples of 3 modes of subduction initiation, one type by induced nucleation of a subduction zone (polarity reversal) and two types of spontaneous nucleation of a subduction zone (transform collapse and plumehead margin collapse). Subduction initiation, either induced or spontaneous, requires a long and deep lithospheric weakness to exploit, perhaps to allow water infiltration and formation of serpentine minerals deep in the lithosphere. Two proposed types of subduction initiation are not well supported by natural observations: transference and passive margin collapse. Even though we have no convincing examples of passive margin collapse, this is might happen along a shear margin. These two "non-examples" must reflect the great strength of normal lithosphere. Further work is needed to expand on and understand the implications of these observations, but for the time being geoscientists doing tectonic or paleogeographic reconstructions should make an effort to honor these constraints.

Acknowledgements

We appreciate comments and criticisms from two anonymous referees, Douwe van Hinsbergen, Fernando Marques, and editor Philippe Agard. This is UTD Geosciences contribution No. 1312.

References

Agard, P., Jolivet, L., Vrielynck, B., Burov, E., Monie, P., 2007. Plate acceleration: the obduction trigger? Earth Planet. Sci. Lett. 258, 428–441.

Agard, P., Yamato, P., Soret, M., Prigent, C., Guillot, S., Plunder, A., Dubacq, B., Chauvet, A., Monie, P., 2016. Plate interface rheological switches during subduction infancy: control on slab penetration and metamorphic sole formation. Earth Planet. Sci. Lett. 451, 208–220.

Alvarez-Marron, J., Rubio, E., Torne, M., 1997. Subduction-related structures in the North Iberian Margin. J. Geophys. Res. B 102, 22,487–22,511.

Amiguet, E., Reynard, B., Caracas, R., Van de Moortele, B., Hilairet, N., Wang, Y.B., 2012. Creep of phyllosilicates at the onset of plate tectonics. Earth Planet. Sci. Lett. 345, 142–150.

Arculus, R.J., Ishizuka, O., Bogus, K.A., Gurnis, M., Hickey-Vargas, R., Aljahdali, M.H., Bandini-Maeder, A.N., Barth, A.P., Brandl, P.A., Drab, L., do Monte Guerra, R., Hamada, M., Jiang, F., Kanayama, K., Kender, S., Kusano, Y., Li, H., Loudin, L.C., Maffione, M., Marsaglia, K.M., McCarthy, A., Meffre, S., Morris, A., Neuhaus, M., Savov, I.P., Sena, C., Tepley III, F.J., van der Land, C., Yogodzhinski, G., Zhang, S., 2015. A record of spontaneous subduction initiation in the Izu–Bonin–Mariana arc. Nat. Geosci. 8, 728–733.

Baes, M., Govers, R., Wortel, R., 2011. Subduction initiation along the inherited weakness zone at the edge of a slab: insights from numerical models. Geophys. J. Int. 184, 991–1008.

Becker, T.W., Faccenna, C., 2011. Mantle conveyor beneath the Tethyan collisional belt. Earth Planet. Sci. Lett. 310, 453–461.

Benioff, Hugo, 1949. Seismic evidence for the fault origin of oceanic deeps. Bull. Geol. Soc. Am. 60, 1837–1866.

Bercovici, D., 2003. The generation of plate tectonics from mantle convection. Earth Planet. Sci. Lett. 205, 107–121.

Bercovici, D., Ricard, Y., 2014. Plate tectonics, damage and inheritance. Nature 508, 513–516.

Burke, K., Dewey, J.F., 1974. Hot spots and continental breakup: implications for collisional orogeny. Geology 2, 57–60.

Burov, E., Cloetingh, S., 2010. Plume-like upper mantle instabilities drive subduction initiation. Geophys. Res. Lett. 37, L03309. http://dx.doi.org/10.1029/2009GL041535.

Carpenter, B.M., Marone, C., Saffer, D.M., 2011. Weakness of the San Andreas Fault revealed by samples from the active fault zone. Nat. Geosci. 4, 251–254.

Casey, J.F., Dewey, J.F., 1984. Initiation of subduction zones along transform and accreting plate boundaries, triple junction evolution and forearc spreading centers: implications for ophiolite geology and obduction. In: Gass, I.G., Lippard, S.J., Shelton, A.W. (Eds.), Ophiolites and Oceanic Lithosphere. Blackwell, London, pp. 83–97.

Chertova, M.V., Spakman, W., Geenen, T., van den Berg, A.P., van Hinsbergen, D.J.J., 2014. Underpinning tectonic reconstructions of the western Mediterranean region with dynamic slab evolution from 3-D numerical modeling. J. Geophys. Res. 119, 5876–5902.

Cloetingh, S., Wortel, M.J.R., Vlaar, N.J., 1982. Evolution of passive continental margins and initiation of subduction zones. Nature 297, 139–142.

Cloetingh, S., Wortel, R., Vlaar, N.J., 1989. On the initiation of subduction zones. Pure Appl. Geophys. 129, 7–25.

Cluzel, D., Aitchison, J.C., Picard, C., 2001. Tectonic accretion and underplating of mafic terranes in the Late Eocene intraoceanic fore-arc of New Caledonia (Southwest Pacific): geodynamic implications. Tectonophysics 340, 23–59.

Coats, R.R., 1962. Magma type and crustal structure in the Aleutian arc. In: The Crust of the Pacific Basin. American Geophysical Union Monograph 6. pp. 92–109.

Collettini, C., Niemeijer, A., Viti, C., Marone, C., 2009. Fault zone fabric and fault weakness. Nature 462, 907–910.

Cooper, P.A., Taylor, B., 1985. Polarity reversal in the Solomon Islands arc. Nature 314, 428–430.

Crameri, F., Tackley, P.J., 2016. Subduction initiation from a stagnant lid and global overturn: new insights from numerical models with a free surface. Progr. Earth Planet. Sci. http://dx.doi.org/10.1186/s40645-016-0103-8.

Crameri, F., Tackley, P.J., Meilick, I., Gerya, T., Kaus, B.J.P., 2012. A free plate surface and weak oceanic crust produce single-sided subduction on Earth. Geophys. Res. Lett. http://dx.doi.org/10.1029/2011GL050046.

Davies, G.F., 1999. Dynamic Earth. Cambridge University Press, New York.

Dickinson, W.R., 2003. The pace and power of myth in geoscience: an Associate Editor's perspective. Am. J. Sci. 303, 856–864.

Dickinson, W.R., Sealey, D.R., 1979. Structure and stratigraphy of forearc regions: The American Association of Petroleum Geologists Bulletin. 63. pp. 2–31.

Dietrich, V., Emmermann, R., Oberhänsli, R., Puchelt, H., 1978. Geochemistry of basaltic and gabbroic rocks from the Mariana basin and the Mariana trench. Earth Planet. Sci. Lett. 39, 127–144.

van Dinther, Y., Gerya, T.V., Dalguer, L.A., Mai, P.M., Morra, G., Giardini, D., 2013. The seismic cycle at subduction thrusts: insights from seismo-thermo-mechanical models. J. Geophys. Res. 118, 1502–1525.

Doin, M.-P., Henry, P., 2001. Subduction initiation and continental crust recycling: the roles of rheology and eclogitization. Tectonophysics 342, 163–191.

Duarte, J.C., Rosas, F.M., Terrinha, P., Schellart, W.P., Boutelier, D., Gutscher, M.A., Ribeiro, A., 2013. Are subduction zones invading the Atlantic? Evidence from the southwest Iberia margin. Geology 41, 839–842.

Duretz, T., Agard, P., Yamato, P., Ducassou, C., Burov, E.B., Gerya, T.V., 2016. Thermo-mechanical modeling of the obduction process based on the Oman Ophiolite case. Gondwana Res. 32, 1–10.

Dymkova, D., Gerya, T., 2013. Porous fluid flow enables oceanic subduction initiation on Earth. Geophys. Res. Lett. 40, 5671–5676.

Erickson, S.G., 1993. Sedimentary loading, lithospheric flexure, and subduction initiation at passive margins. Geology 21, 125–128.

Erickson, S.G., Arkani-Hamed, J., 1993. Subduction initiation at passive margins: the Scotian basin, Eastern Canada as a potential example. Tectonics 12, 678–687.

Escartín, J., Hirth, G., Evans, B., 1997. Nondilatant brittle deformation of serpentinites: implications for Mohr-Coulomb theory and the strength of faults. J. Geophys. Res. 102, 2897–2913.

Escartín, J., Hirth, G., Evans, B., 2001. Strength of slightly serpentinized peridotites: implications for the tectonics of oceanic lithosphere. Geology 29, 1023–1026.

Faccenda, M., Gerya, T.V., Chakraborty, S., 2008. Styles of post-subduction collisional orogeny: influence of convergence velocity, crustal rheology and radiogenic heat production. Lithos 103, 257–287.

Faccenna, C., Giardini, D., Devy, P., Argentiri, A., 1999. Initiation of subduction at Atlantic-type margins: insights from laboratory experiments. J. Geophys. Res. 104, 2749–2766.

Forsythe, D., Uyeda, S., 1975. On the relative importance of the driving forces of plate motion. Geophys. J. R. Astron. Soc. 43, 163–200.

Fryer, P., Pearce, J.A., 1992. Introduction to the scientific results of Leg 125. Proc. Ocean Drill. Program Sci. Results 125, 3–11.

Fyfe, W.S., Leonardos Jr., O.H., 1977. Speculations on the causes of crustal rifting and subduction, with applications to the Atlantic margin of Brazil. Tectonophysics 42, 29–36.

Gerya, T., 2011. Future directions in subduction modeling. J. Geodyn. 52, 344–378.

Gerya, T.V., Yuen, D.A., 2003. Rayleigh-Taylor instabilities from hydration and melting propel "cold plumes" at subduction zones. Earth Planet. Sci. Lett. 212, 47–62.

Gerya, T.V., Connolly, J.A.D., Yuen, D.A., 2008. Why is terrestrial subduction one-sided? Geology 36 (1), 43–46.

Gerya, T., Stern, R.J., Baes, M., Sobolev, S., Whattam, S., 2015. Plume-induced subduction initiation triggered plate tectonics on Earth. Nature 527, 221–225.

Goren, L., Aharonov, E., Mulugeta, G., Koyi, H.A., Mart, Y., 2008. Ductile deformation of passive margins: a new mechanism for subduction initiation. J. Geophys. Res. 113, B08411.

Gurnis, M., Hall, C., Lavier, L., 2004. Evolving force balance during incipient subduction. Geochem. Geophys. Geosyst. 5, Q07001. http://dx.doi.org/10.1029/2003GC000681.

Gutenberg, B., Richter, C.F., 1938. Depth and geographical distribution of deep-focus earthquakes. Geol. Soc. Am. Bull. 49, 249–288.

Gutscher, M.-A., Malod, J., Rehault, J.-P., Contrucci, I., Klingelhoefer, F., Mendes-Victor, L., Spakman, W., 2002. Evidence for active subduction beneath Gibraltar. Geology 30, 1071–1074.

Gutscher, M.-A., Dominguez, S., Westbrook, G.K., Le Roy, P., Rosas, F., Duarte, J.C., Terrinha, P., Miranda, J.M., Graindorge, D., Gailler, A., Sallares, V., Bartolome, R., 2012. The Gibraltar subduction: a decade of new geophysical data. Tectonophysics 574–575, 72–91.

Hall, C.E., Gurnis, M., Sdrolias, M., Lavier, L.L., Muller, R.D., 2003. Catastrophic initiation of subduction following forced convergence across fractures zones. Earth Planet. Sci. Lett. 212, 15–30.

Hamilton, W., 1969. Mesozoic California and the underflow of Pacific mantle. Bull. Geol. Soc. Am. 80, 2409–2428.

Hansen, V.L., 2009. Subduction origin on early Earth: a hypothesis. Geology 35, 1059–1062.

Hilairet, N., Reynard, B., Wang, Y., Daniel, I., Merkel, S., Nishiyama, N., Petitgirard, S., 2007. High-pressure creep of serpentine, interseismic deformation, and initiation of subduction. Science 318, 1910–1913.

van Hinsbergen, D.J.J., Peters, K., Maffione, M., Spakman, W., Guilmette, C., Thieulot, C.,

Plümper, O., Gürer, D., Brower, F.M., Aldanmaz, E., Kymakci, N., 2015. Dynamics of intraoceanic subduction initiation: 2. Suprasubduction zone ophiolite formation and metamorphic sole exhumation in context of absolute plate motions. Geochem. Geophys. Geosyst. 16, 1771–1785. http://dx.doi.org/10.1002/2015GC005745.

Hirauchi, K., Fukushima, K., Kido, M., Muto, J., Okamoto, A., 2016. Reaction-induced rheological weakening enables oceanic plate subduction. Nat. Commun. 7, 12550.

House, M.A., Gurnis, M., Kamp, P.J.J., Sutherland, R., 2002. Uplift in the Fiordland region, New Zealand: implications for incipient subduction. Science 297, 2038–2041.

Hussong, D.M., Uyeda, S., Knapp, R., Ellis, H., Kling, S., Natland, J., 1982. 1. Deep Sea Drilling Project Leg 60: cruise objectives, principal results, and explanatory notes. In: Initial Reports of the Deep Sea Drilling Project, Leg 60, pp. 1–30.

Isacks, B., Oliver, J., Sykes, L.R., 1968. Seismology and the new global tectonics. J. Geophys. Res. 73, 5855–5899.

Ishizuka, O., Tani, K., Reagan, M.K., Kanayama, K., Umino, S., Harigane, Y., Sakamoto, I., Miyajima, Y., Yuasa, M., Dunkley, D.J., 2011. The timescales of subduction initiation and subsequent evolution of an oceanic island arc. Earth Planet. Sci. Lett. 306, 229–240.

Iyer, K., Rüpke, L.H., Morgan, J.P., Grevemeyer, I., 2012. Controls of faulting and reaction kinetics on serpentinization and double Benioff zones. Geochem. Geophys. Geosyst. 13. http://dx.doi.org/10.1029/2012GC004304.

Karig, D.E., 1982. Initiation of subduction zones: implications for arc evolution and ophiolite development. In: Leggett, J.K. (Ed.), Trench-Forearc Geology. Geol. Soc. Spec. Publ. 10. pp. 563–576 edited by.

Kemp, D.V., Stevenson, D.J., 1996. A tensile, flexural model for the initiation of subduction. Geophys. J. Int. 125, 73–93.

Korenaga, J., 2007. Thermal cracking and the deep hydration of oceanic lithosphere: a key to the generation of plate tectonics? J. Geophys. Res. 112 (B05), 408.

Korenaga, J., 2013. Initiation and evolution of plate tectonics on Earth: theories and observations. Annu. Rev. Earth Planet. Sci. 41, 117–151.

Le Pichon, X., 1968. Sea-floor spreading and continental drift. J. Geophys. Res. 73, 3661–3697.

Le Pichon, X., Sibuet, J.-C., 1971. Western extension of boundary between European and Iberian plates during the Pyrenean orogeny. Earth Planet. Sci. Lett. 12, 83–88.

Lebrun, J.-F., Lamarche, G., Collot, J.-Y., 2003. Subduction initiation at a strike-slip plate boundary: the Cenozoic Pacific-Australian plate boundary, south of New Zealand. J. Geophys. Res. 108 (B9), 2453. http://dx.doi.org/10.1029/2002JB002041.

Leng, W., Gurnis, M., 2015. Subduction initiation at relic arcs. Geophys. Res. Lett. 42, 7014–7021. http://dx.doi.org/10.1002/2015GL064985.

Leng, W., Gurnis, M., Asimow, P., 2012. From basalts to boninites: the geodynamics of volcanic expression during induced subduction initiation. Lithosphere 4, 511–523.

Lithgow-Bertelloni, C., 2014. Driving forces: slab pull, ridge push. In: Encyclopedia of Marine Geosciences.

Lu, G., Kaus, B.J.P., Zhao, L., Zheng, T., 2015. Self-consistent subduction initiation induced by mantle flow. Terra Nova 27 (2), 130–138.

Lus, W.Y., McDougall, I., Davies, H.L., 2004. Age of the metamorphic sole of the Papuan Ultramafic Belt ophiolite, Papua New Guinea. Tectonophysics 392, 85–101.

Maffione, M., Thieulot, C., van Hinsbergen, D.J.J., Morris, A., Plümper, O., Spakman, W., 2015. Dynamics of intraoceanic subduction initiation: 1. Oceanic detachment fault inversion and the formation of supra-subduction zone ophiolites. Geochem. Geophys. Geosyst. 16, 1753–1770. http://dx.doi.org/10.1002/2015GC005746.

Maffione, M., van Hinsbergen, D.J.J., de Gelder, G.I.N.O., van der Goes, F.C., Morris, A., 2017. Kinematics of Late Cretaceous subduction initiation in the Neo-Tethys Ocean reconstructed from ophiolites of Turkey, Cyprus, and Syria. J. Geophys. Res. 122, 3953–3976.

Marques, F.O., 2010. Comment on “Deep structure, recent deformation and analogue modeling of Cadiz accretionary wedge: implications for the 1755 Lisbon earthquake”, by Gutscher et al. 2009. Tectonophysics 485, 327–329.

Marques, F., Kaus, B.J.P., 2016. Speculations on the impact of catastrophic subduction initiation on the Earth system. J. Geodyn. 93, 1–16.

Marques, F.O., Nikolaeva, K., Assumpcao, M., Gerya, T.V., Bezerra, F.H.R., do Nascimento, A.F., Ferreira, J.M., 2013. Testing the influence of far-field topographic forcing on subduction initiation at a passive margin. Tectonophysics 608, 517–524.

Marques, F.O., Cabral, F.R., Gerya, T.V., Zhu, G., May, D.A., 2014. Subduction initiates at straight passive margins. Geology 42, 331–334.

Matsumoto, T., Tomoda, Y., 1983. Numerical-simulation of the initiation of subduction at the fracture-zone. J. Phys. Earth 31, 183–194.

McKenzie, D.P., 1977. The initiation of trenches: a finite amplitude instability. In: Talwani, M., Pittman, W.C. (Eds.), Island Arcs, Deep Sea Trenches, and Back-Arc Basins. Maurice Ewing Ser. I. AGU, Washington, D.C., pp. 57–61.

McKenzie, D.L., Parker, R.L., 1967. The North Pacific: an example of tectonics on a sphere. Nature 216, 1276–1280.

Melhuish, A., Sutherland, R., Davey, F.J., Lamarche, G., 1999. Crustal structure and neotectonics of the Puysegur oblique subduction zone, New Zealand. Tectonophysics 313, 335–362.

Menzies, M.A., Klemperer, S.L., Ebinger, C.J., Baker, J., 2002. Characteristics of volcanic rifted margins. Geol. Soc. Am. Spec. Pap. 362, 1–14.

Moghadam, H.S., Corfu, F., Stern, R.J., 2013. U-Pb zircon ages of Late Cretaceous Nain-Dehshir ophiolites, central Iran. J. Geol. Soc. Lond. 170, 175–184.

Monié, P., Agard, P., 2009. Coeval blueschist exhumation along thousands of kilometers: implications for subduction channel processes. Geochem. Geophys. Geosyst. 7, Q07002.

Moore, D.E., Lockner, D.A., 2007. Comparative deformation behavior of minerals in serpentinized ultramafic rock: application to the slab-mantle interface in subduction zones. Int. Geol. Rev. 49, 401–415.

Moore, D.E., Lockner, L.D.A., Summers, R., Shengli, M., Byerlee, J.D., 1996. Strength of chrysotile-serpentinite gouge under hydrothermal conditions: can it explain a weak San Andreas fault? Geology 24, 1041–1044.

Morishita, T., Tani, K., Shukuno, H., Harigane, Y., Tamura, A., Kumagi, H., Hellebrand, E., 2011. Diversity of melt conduits in the Izu-Bonin-Mariana forearc mantle: implications for the earliest stage of arc magmatism. Geology 39, 411–414.

Mueller, S., Phillips, R.J., 1991. On the initiation of subduction. J. Geophys. Res. 96, 651–665.

Müller, R.D., Seton, M., Zahirovic, S., Williams, S.E., Matthews, K.J., Wright, N.M., Shephard, G.E., Maloney, K.T., Barnett-Moore, N., Hosseinpour, M., Bower, D.J., Cannon, J., 2016. Ocean basin evolution and global-scale plate reorganization events since Pangea breakup. Annu. Rev. Earth Planet. Sci. 44, 107–138.

Natland, J.H., Tarney, J., 1982. Petrologic evolution of the Mariana arc and Back-arc basin system — a synthesis of drilling results in the South Philippine sea. Initial Rep. Deep Sea Drill. Proj. 60, 877–908 (US Gov't. Printing Office, Washington DC).

Nikolaeva, K., Gerya, T.V., Connolly, J.A.D., 2008. Numerical modelling of crustal growth in intraoceanic volcanic arcs. Phys. Earth Planet. Inter. 171, 336–356.

Nikolaeva, K., Gerya, T.V., Marques, F.O., 2010. Subduction initiation at passive margins: numerical modeling. J. Geophys. Res. 115, B03406.

Nikolaeva, K., Gerya, T.V., Marques, F.O., 2011. Numerical analysis of subduction initiation risk along the Atlantic American passive margins. Geology 39, 463–466.

Niu, Y., O'Hara, M.J., Pearce, J.A., 2003. Consequence of lateral compositional buoyancy contrast within the lithosphere: a petrological perspective. J. Petrol. 44, 851–866.

Pearce, J.A., Lippard, S.J., Roberts, S., 1984. Characteristics and tectonic significance of supra-subduction zone ophiolites. Geol. Soc. Lond., Spec. Publ. 16, 77–94.

Platt, J., Houseman, G., Gutscher, M.-A., Malod, J., Rehault, J.-P., Contrucci, I., Klinghoefer, F., Mendes-Victor, L., Spakman, W., 2003. Evidence for active subduction beneath Gibraltar: comment and reply. Geology 31. http://dx.doi.org/10.1130/0091-7613-31.1.e22.

Platt, J.P., Behr, W.M., Johanesen, K., Williams, J.R., 2013. The Betic-Rif arc and its orogenic hinterland: a review. Annu. Rev. Earth Planet. Sci. 41, 313–357.

Pubellier, M., Monnier, C., Maury, R., Tamayo, R., 2004. Plate kinematics, origin and tectonic emplacement of supra-subduction ophiolites in SE Asia. Tectonophysics 392, 9–36.

Pysklywek, R.N., 2001. Evolution of subduction mantle lithosphere at a continental plate boundary. Geophys. Res. Lett. 23, 4399–4402.

Reagan, M.K., Ishizuka, O., Stern, R.J., Kelley, K.A., Ohara, Y., Blichert-Toft, J., Bloomer, S.H., Cash, J., Fryer, P., Hanan, B.B., Hickey-Vargas, R., Ishii, T., Kimura, J.I., Peate, D.W., Rowe, M.C., Woods, M., 2010. Fore-arc basalts and subduction initiation in the Izu-Bonin-Mariana system. Geochem. Geophys. Geosyst. 11, Q03X12. http://dx.doi.org/10.1029/2009GC002871.

Reagan, M.K., Pearce, J.A., Petrnotis, K., Avery, A.J., Carvallo, C., Chapman, T., Christeson, G.L., Ferré, E.C., Godard, M., Heaton, D.E., Kirchenbaur, M., Kurz, W., Kutterolf, S., Li, H., Li, Y., Michibayashi, K., Morgan, S., Nelson, W.R., Prytulak, J., Python, M., Robertson, A.H.F., Ryan, J.G., Sager, W.W., Sakuyama, T., Shervais, J.W., Shimizu, K., Whattam, S.A., 2017. Subduction initiation and ophiolite crust: new insights from IODP drilling. Int. Geol. Rev (in press).

Reay, A., Parkinson, D., 1997. Adakites from Solander Island, New Zealand. J. Geol. Geophys. 40, 121–126.

Regenauer-Lieb, K., Yuen, D.A., Branlund, J., 2001. The initiation of subduction: critically by addition of water? Science 294, 578–580.

Reinen, L.A., 2000. Seismic and aseismic slip indicators in serpentinite gouge. Geology 28, 135–138.

Reinen, L.A., Weeks, J.D., Tullis, T.E., 1994. The frictional behavior of lizardite and antigorite serpentinites: experiments, constitutive models, and implications for natural faults. Pure Appl. Geophys. 143, 318–358.

Resing, J.A., Rubin, K.H., Embley, R.W., Lupton, J., Baker, E., Dziak, R., Baumberger, T., Lilley, M., Huber, J., Shank, T.M., Butterfield, D., Clague, D., Keller, N., Merle, S., Buck, S.J., Michael, P., Soule, A., Caress, D.W., Walker, R.S.L., Davis, R., Cowen, J.R., Reysenbach, A.-L., Thomas, H., 2011. Active submarine eruption of boninite at West Mata Volcano in the extensional NE Lau Basin. Nat. Geosci. 44, 799–806.

Rey, P.F., Coltice, N., Flament, N., 2014. Spreading continents kick-started plate tectonics. Nature 513, 405–408.

Rolf, T., Tackley, P.J., 2011. Focusing of stress by continents in 3D spherical mantle convection with self-consistent plate tectonics. Geophys. Res. Lett. 38, L18301. http://dx.doi.org/10.1029/2011GL048677.

Ruiz, M., Díaz, J., Pedreira, D., Gallart, J., Pulgar, J.A., 2017. Tectonophysics 717, 65–82.

Schmeling, H., Babeyko, A.Y., Enns, A., Faccenna, C., Funiciello, F., Gerya, T., Golabek, G.J., Grigull, S., Kaus, B.J.P., Morra, G., Schmalholz, S.M., van Hunen, J., 2008. Benchmark comparison of spontaneous subduction models — towards a free surface. Phys. Earth Planet. Inter. 171, 198–223.

Shemenda, A.I., 1992. Horizontal lithosphere compression and subduction: constraints provided by physical modelling. J. Geophys. Res. 97, 11097–11116.

Shemenda, A.I., 1993. Subduction of the lithosphere and back arc dynamics: insights from physical modelling. J. Geophys. Res. 98, 16167–16185.

Solomatov, V.S., 2004. Initiation of subduction by small-scale convection. J. Geophys. Res. 109 (B1). http://dx.doi.org/10.1029/2003JB002628.

Stern, R.J., 2004. Subduction initiation: spontaneous and induced. Earth Planet. Sci. Lett. 226, 275–292.

Stern, R.J., Bloomer, S.H., 1992. Subduction zone infancy: examples from the Eocene Izu-Bonin-Mariana and Jurassic California arcs. Geol. Soc. Am. Bull. 104, 1621–1636.

Stern, R.J., Reagan, M., Ishizuka, O., Ohara, Y., Whattam, S., 2012. To understand subduction initiation, study forearc crust; to understand forearc crust, study ophiolites. Lithosphere 4, 469–483.

Stern, R.J., Lieu, W., Manley, A., Ward, A., Fechter, T., Farrar, E., McComber, S., Windler, J., 2017a. A new animation of subduction zone processes developed for the undergraduate and community college audience. Geosphere 13, 628–643.

Stern, R.J., Gerya, T., Tackley, P.J., 2017b. Stagnant lid tectonics: perspectives from

silicate planets, dwarf planets, large moons, and large asteroids. Geosci. Front. http://dx.doi.org/10.1016/j.gsf.2017.06.004.
Sutherland, R., Barnes, P., Uruski, C., 2006. Miocene-Recent deformation, surface elevation, and volcanic intrusion of the overriding plate during subduction initiation, offshore southern Fiordland, Puysegur margin, southwest New Zealand. N. Z. J. Geol. Geophys. 49, 131–149.
Tackley, P.J. 2000. Self-consistent generation of tectonic plates in time-dependent, three dimensional mantle convection simulations. Part 1: pseudo-plastic yielding: Geochem. Geophys. Geosyst., v. 1, paper no. 2000GC000036.
Taylor, B., Goodliffe, A.M., 2004. The West Philippine Basin and the initiation of subduction, revisited. Geophys. Res. Lett. 31, L12602. http://dx.doi.org/10.1029/2004GL020136.
Tetreault, J.L., Buiter, S., 2012. Geodynamic models of terrane accretion: testing the fate of island arcs, oceanic plateaus, and continental fragments in subduction zones. J. Geophys. Res. 117, B08403.
Thiebot, E., Gutscher, M.-A., 2006. The Gibraltar Arc seismogenic zone (part 1): constraints on a shallow east dipping fault plane source for the 1755 Lisbon earthquake provided by seismic data, gravity and thermal modeling. Tectonophysics 426, 135–152.
Thielmann, M., Kaus, B.J.P., 2012. Shear heating induced lithospheric localization: does it result in subduction? Earth Planet. Sci. Lett. 359–360, 1–13.
Toth, J., Gurnis, M., 1998. Dynamics of subduction initiation at preexisting fault zones. J. Geophys. Res. 103 (B8), 18,053–18,067.
Turcotte, D.L., Ahern, J.L., Bird, J.M., 1977. The state of stress at continental margins. Tectonophysics 42, 1–28.
Ueda, K., Gerya, T., Sobolev, S.V., 2008. Subduction initiation by thermal-chemical plumes: numerical studies. Phys. Earth Planet. Inter. 171, 296–312.
Ulvrova, M., Williams, S., Coltice, N., Tackley, P., 2017. Where does subduction initiate and die? Insights from global convection models with continental drift. In: EGU General Assembly Conference Abstracts 19. pp. 15,780.
Uyeda, S., Ben-Avraham, Z., 1972. Origin and development of the Philippine Sea. Nat. Phys. Sci. 240, 176–178.
Van der Lee, S., Regenauer-Lieb, K., Yuen, D.A., 2008. The role of water in connecting past and future episodes of subduction. Earth Planet. Sci. Lett. 273, 15–27.
Vlaar, N.J., Wortel, M.J.R., 1976. Lithospheric aging, instability and subduction. Tectonophysics 32, 331–351.
Vogt, K., Gerya, T.V., 2014. From oceanic plateaus to allochthonous terranes: numerical modelling. Gondwana Res. 25, 494–508.
Wadati, K., 1928. Shallow and deep earthquakes. Geophys. Mag. 1, 161–202.
Wakabayashi, J., Dilek, Y., 2003. What constitutes 'emplacement' of an ophiolite?: mechanisms and relationship to subduction initiation and formation of metamorphic soles. In: Dilek, Y., Robinson, P.T. (Eds.), Ophiolites in Earth History. Geological Society, London Special Publication 218. pp. 427–447.
Whattam, S.A., Stern, R.J., 2011. The 'subduction initiation rule': a key for linking ophiolites, intra-oceanic forearcs and subduction initiation. Contrib. Mineral. Petrol. 162, 1031–1045.
Whattam, S., Stern, R.J., 2015. Late Cretaceous plume-induced subduction initiation along the southern and eastern margins of the Caribbean: the first documented example with implications for the onset of plate tectonics. Gondwana Res. 27, 38–63.
White, D.A., Roeder, D.H., Nelson, T.H., Crowell, J.C., 1970. Subduction. Geol. Soc. Am. Bull. 81, 3431–3432.
Wilson, J.T., 1966. Did the Atlantic close and then re-open? Nature 211, 676–681.
Zheng, L., May, D., Gerya, T., Bostock, M., 2016. Fluid-assisted deformation of the subduction interface: coupled and decoupled regimes from 2-D hydromechanical modeling. J. Geophys. Res. 121, 6132–6149.
Zhou, X., Gerya, T., Li, Z., Stern, R.J., 2016. Dynamics of intraoceanic subduction initiation: 2D thermomechanical modeling. In: AGU 2016 Fall Meeting, Abstract T31C-2919.
Zhu, G., Gerya, T.V., Yuen, D.A., Honda, S., Yoshida, T., Connolly, J.A.D., 2009. 3-D Dynamics of hydrous thermalchemical plumes in oceanic subduction zones. Geochem. Geophys. Geosyst. 10, Q11006.